Chapter 4

MANGANESE DIOXIDE BASED SUPERCAPACITORS

Chengjun Xu[*] and Shan Shi

Advanced Materials Institute, Graduate School at Shenzhen, Tsinghua
University, Shenzhen City, Guangdong Province, China

ABSTRACT

The increasing worldwide interest in MnO_2 for supercapacitor applications is based on anticipation that MnO_2 based high-voltage aqueous supercapacitors will ultimately serve as safety and low cost alternative to state-of-the-art commercial organic EDLC or RuO_2-based acid systems.

In this chapter, the crystalline structure features, synthesis method, charge storage mechanism of MnO_2 as well as the current status of MnO_2 based supercapacitors are summarized and introduced in detail.

1. INTRODUCTION

Energy is always the priority issue for human beings. In 21st century, as the end of fossil fuel era is getting close, the problem of pollution due to combustion of fossil fuel has become worldwide. The renewable and clean

---

[*] Corresponding E-mail: C. Xu (vivaxuchengjun@163.com).

energy sources as well as efficient use of energy are highly necessary to make our economy, environment, society, and human species sustainable. Energy storage technology, an intermediate step, is a new approach to the versatile usage of energycleanly and efficiently. Hence, energy storage devices with high capacitance and power have been received more concerns and interesting. Supercapacitors can provide high power density (higher than a few kW kg^{-1}) and moderate energy density.

It is also characterized with environmental friendliness, high safety, and good efficiency and can be operated in a wide temperature range with a near-infinite long cycle life. Thus, supercapacitors have being applied in communications, transportation, consumer electronics, aviation, or related technologies [1-3].

Normally, supercapacitor consists of a pair of ideally polarizable electrodes, which are immersed in an electrolyte and physically separated by a porous membrane. If electrochemically active materials of both electrodes are identically the same, it will be a symmetric supercapacitor, otherwise, it is an asymmetric one. The energy stored in such devices is calculated by E=1/2 CV^2, where C is capacitance and V is operating voltage across the electrodes. The capacitance of a supercapacitor is determined by the specific capacitance of both electrodes, which is normally hundreds of Farad per gram (F g^{-1}). Operating voltage of a supercapacitor is another vital parameter, which is determined by the decomposition of electrolytes as well as the width of electrochemical potential window of positive and negative electrodes, respectively. For the symmetric supercapacitor, it generally has a voltage of 1 V in aqueous electrolytes and 2.5 V in an organic system. An even higher voltage of up to 4.0 V can be achieved for recent ionic-liquid-based systems or so-called asymmetric design [4]. High voltage organic systems can store more energy, but deliver lower power than inorganic systems. The electronic conductivity of organic electrolytes is relatively low. Moreover, flammable and expensive organic electrolytes will cause the safety and cost issues.

The first supercapacitor [5] was invented in 1957 and later known as electric double layer capacitor (EDLC), which consists of two identical electrodes fabricated from active porous carbon material, conductive agents and a binder. Porous carbon materials possess a large surface area exceeding 2000 m^2 g^{-1}, onto which charge is stored electrostatically through the reversible adsorption of ions of the electrolyte. Since the capacitance is proportional to the surface area of electrode accessible to the ions, large surface area material renders EDLC to store hundreds or even thousands of times more charges (tens to hundreds of F g^{-1}) than electrolytic capacitors [3].

Subsequently, a so-called pseudo-capacitive supercapacitor was proposed, in which the charge storage is not electrostatic, but occurs through a charge transfer from redox reaction. This process is a redox faradic reaction, but the behavior just likes a capacitor and possesses all features and advantages of the supercapacitor. Metal oxides or hydrous, such as Ru, Co, Mn oxides/hydroxide, and conductive polymers, for instance polyaniline and polypyrrole, are materials with psuedocapacitive properties. The capacitance of materials based on psuedocapacitive reactions can reach to one thousand farad per gram, 10~100 times higher than porous carbon. For example, RuO_2 is well known because of its enormous specific capacitance of 1000 F g^{-1} [6]. RuO_2 exhibits excellent electrochemical performance with large specific capacitance and good stability. However, ruthenium is a very expensive material and a rare element. Thus, considerable efforts have been made for the development of inexpensive transition metal oxides such as NiO, V_2O_5, and MnO_2 etc., [7-9].

MnO_2 chemistry has being widely attracted. The intense interest in MnO_2 for energy storage applications comes from its low cost, non-toxicity and abundance in raw materials. Dating back to the work of Leclanché in the 1860s, MnO_2 has long been used in primary Zn/MnO_2 alkaline cells. In such cells, MnO_2 (typically in γ phase) serves as an active cathode material. After the invention of lithium ion batteries, MnO_2 or spinel $Li_{1-x}MnO_2$ were also used as cathode materials. In 1999, the use of MnO_2 for electrochemical energy storage continued to expand to a new area, electrochemical supercapacitor.

Lee and Goodenough initially reported that amorphous MnO_2 electrodes exhibited a capacitor-like electrochemical response in mild aqueous electrolyte and delivered a specific capacitance of about 200 F g^{-1} [9]. Since that, interest in MnO_2 as active material for supercapacitor has being grown steadily. Subsequently Hong [10] et al., designed a MnO_2-based aqueous asymmetric capacitor with 2 V operating voltage, two times of that of symmetric aqueous capacitor.

The increasing worldwide interest in MnO_2 is based on the anticipation in which MnO_2 will serve as a low-cost electrode material and MnO_2-based high-voltage aqueous supercapacitors will ultimately serve as safe and low-cost alternative to state-of-the-art commercial organic EDLC or RuO_2-based acid systems.

In this chapter, we will address the current status and recent progress in MnO_2 and MnO_2-based supercapacitors with respect to aqueous systems and discuss their future challenges and opportunities.

2. CRYSTALLINE STRUCTURES OF MNO$_2$

MnO_2 represents a general class of materials exhibiting a rich chemistry. MnO_2 is a very interest and attractive material because it is diverse in crystalline structure and rich in Mn valence. Normally MnO_2 is a complex and non-stoichiometric oxide and often contains foreign cations, physisorbed and structural water moleculars, and structural vacancies. Due to the presence of foreign species, the average valence of Mn in MnO_2 generally locates between 3 and 4. However, the variety of MnO_2 in structure and valence comes from only one basic structural unit, MnO_6 octahedron. It just likes string in a string theory world. In a MnO_2 world, this little tiny MnO_6 octahedron enables the buildup of a colorful and diverse world, in which every version is just one kind of the combinations of MnO_6octahedra. The combination of MnO_6 octahedra provides a veritable "toolbox" [11], from which to design, optimize and synthesize for a specific purpose. Therefore, it is necessary to give a brief review on crystalline structures of MnO_2.

MnO_6 octahedra can share vertices and edges to form endless chains of MnO_6 octahedra subunits, which can in turn be linked to neighboring octahedral chains by sharing corners or edges. The piling up of MnO_6 units enables the building of one dimension (1D), two dimension (2D) or three dimension (3D) tunnels, as shown in Figure 1.
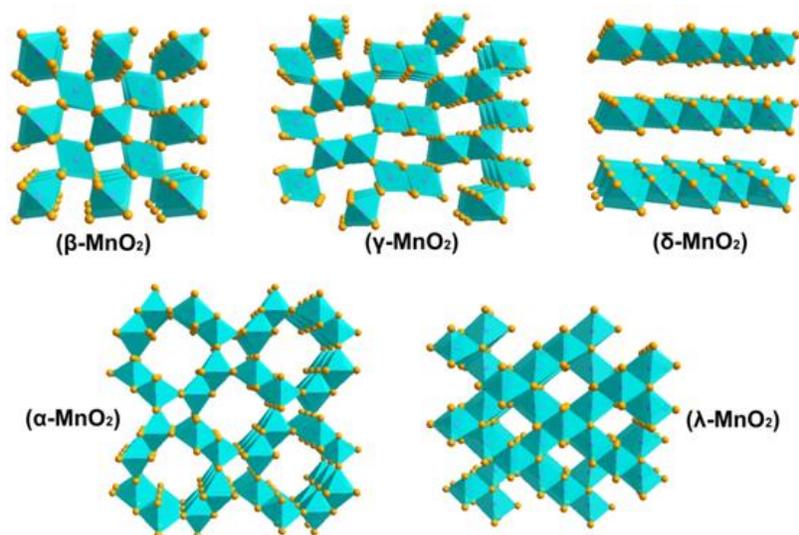

Figure 1. Crystallographic structures of MnO_2.

The different structures could be described by the size of their tunnel determined by the number of octahedral subunits T($n{\times}m$). As shown in Figure 1, the representative 1D tunnel structures include pyrolusite ($T_{1,1}$), ramsdellite ($T_{1,2}$), and hollandite ($T_{2,2}$). The famous 2D structure is birnessite ($T_{1,\infty}$) with a lamellar structure, in which the space distance between two layers ranges from 0.55 to 1.00 nm depending on the presence of foreign cations or water molecular. Spinel λ-MnO_2 is known as 3D tunnel [12, 13].

Typically, and in nature, these tunnels of MnO_2 can be filled with foreign cations, or water molecular. There are many types of MnO_2 containing various univalent and bivalent cations in its tunnels occurring in minerals. For example, alpha MnO_2 (α-MnO_2) groups with 1D structure possess a large open tunnel structure including holladite group (Mg, Ca, Ba, K) Mn_8O_{16}, psilomelane group (Ca, Ba, K) $Mn_5O_{10}{\cdot}H_2O$ and todorokite group (Mn, Ca, Mg) $Mn_3O_7{\cdot}H_2O$. 2D birnessite group minerals include chalcophanite $ZnMn_3O_7{\cdot}3H_2O$, buserite (Ca, Na) $Mn_7O_{14}{\cdot}3H_2O$ and ranceite (Ca, Mn) $Mn_4O_9{\cdot}3H_2O$. And λ-MnO_2 group with 3D tunnel include hetaerolite $ZnMn_2O_4$, hydroehetaerolite $Zn_2Mn_4O_{18}{\cdot}H_2O$ etc. The foreign cations located in the tunnels of manganese dioxides will force Mn^{4+} ions to become Mn^{3+} ion to balance the charge [12]. This cation-containing feature coupled with the reversible transition between Mn(III) and Mn(IV) enables MnO_2 to be used as the relatively ideal material for electrochemical energy storage.

The combination of MnO_2 octahedra with different foreign cations in tunnel gives researchers multiple choices to design and synthesize specific MnO_2 materials for a specific purpose. For example, you can synthesize different tunnel structures to store electrons and electrolyte cations for supercapacitor applications. You can synthesize MnO_2 with or without foreign cations. The species of foreign cation in tunnels also could be different or replaced by others.

Hydration or dehydration also can be accomplished by soaking in water or heat treatment. MnO_2 with above-mentioned specific features could be easily synthesized by controlling the parameters of synthesis procedure.

3. TUNNEL STORAGE PARTICULARITY AND CHARGE STORAGE MECHANISM

The history of MnO_2 for electrochemical energy can be tracked to over 100 years ago in a primary Zn/MnO_2 cell, which dominated in primary battery

chemistry over the century. In such cells, MnO_2 is used as cathode in the aqueous electrolytes and stores charge by a so-called double injection process, which involves in the insertion of protons from the aqueous solutions and the reduction of Mn in oxides by electrons from external circuit [11, 14]. This first step of the double injection process is expressed as following equation:

$$MnO_2 + H^+ + e^- \rightarrow MnOOH \tag{1}$$

If the electrode continues to discharge, MnOOH could be further reduced at the second step:

$$MnOOH + 3H^+ + e^- \rightarrow Mn^{2+} + 2H_2O \tag{2}$$
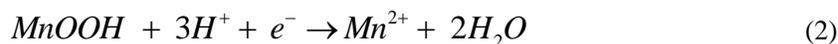
As the ever-increasing needs in energy density of advanced consumer electronics and related technologies, high voltage secondary lithium ion batteries (LIB) have attracted more concerns. MnO_2 materials with 1D, 2D and 3D structures have been studies as cathode materials for LIB, and spinel $Li_{1-x}MnO_2$ has been commercialized for mass production. In such case, the charge storage of MnO_2 in an organic electrolyte is considered as following in the process of equation 3:

$$xLi^+ + xe^- + MnO_2 \leftrightarrow Li_xMnO_2 \tag{3}$$

Lithium cation from the electrolyte diffuses and stores in the tunnels of MnO_2, meanwhile electrons travel to the neighboring Mn (IV) sites to balance the charge [15, 16]. Correspondingly, Mn (IV) ions become Mn (III) and electrons are stored. The insertion process of lithium ions and variation of Mn valence between Mn (IV) and Mn (III) is totally reversible.

As soon as the discovery of capacitive behavior of MnO_2 in the mild aqueous electrolytes, the researchers have been seriously considered the capacitive charge storage mechanism. Since the behaviors of MnO_2 in Zn/MnO_2 cells and RuO_2 in the acid electrolyte are both related to the insertion of protons, some researchers (Pang and Hu) [17, 18] proposed that the capacitive charge storage mechanism of MnO_2 is similar to that of RuO_2 or MnO_2 in Zn/MnO_2 cells expressed as below equation:

$$MnO_x(OH)_y + \delta H^+ + \delta e^- \leftrightarrow MnO_{x-\delta}(OH)_{y+\delta} \qquad (4)$$

This process involves the reversible insertion/desertion of protons and variation of Mn valence between Mn (IV) and Mn (III).

However, some phenomena, in which the specific capacitance of MnO_2 was directly affected by the species and concentrations of the alkaline metal cations with a same pH value, indicated that the charge storage mechanism is not as simple as expressed by equation 4. The earlier clues can be found in the first paper and following papers [9, 19], where it is suggested that the specific capacitance of MnO_2 depends on the nature of Li^+, Na^+, or K^+. In order to demonstrate these phenomena, the chemisorption of alkaline metal cations on the surface of MnO_2 as well as hydrated cations were thought to be important factors. Therefore, a mechanism based on the surface adsorption of the electrolyte cations can be described by:

$$\left(MnO_2\right)_{surface} + M^+ + e^- \leftrightarrow \left(MnO_2 - M^+\right)_{surface} \qquad (5)$$

where M^+ is the alkaline metal cations (Li^+, Na^+, or K^+).

Following researches on the role of the species and concentration of the electrolyte cations indicated a logarithmic dependence of capacitance of MnO_2 on alkaline metal cation activity [20, 21], which demonstrated that alkaline metal cations play an important role in the charge storage process. Later, Bélanger et al., calculated a specific surface capacitance of 110 μF cm^{-2} based on the assumption that a purely faradic charge-transfer storage mechanism is limited to the surface of MnO_2. They had also summarized the data from published reports and found that the most of samples showed a higher specific surface capacitance [22]. The results exhibited that the alkaline metal cations can intercalacte/deintercalate within the oxide lattice during redox process.

$$MnO_2 + xM^+ + xe^- \leftrightarrow M_xMnO_2 \qquad (6)$$
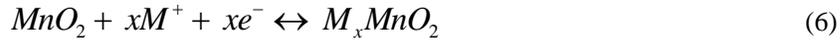
Where M^+ represents alkaline metal cations (Li^+, Na^+, or K^+). Considering the unique tunnel structure of MnO_2, Bélanger et al., also initially proposed a tunnel storage mechanism of the alkaline metal cations in MnO_2 [23].

Many clues have led researchers to understand the charge storage mechanism of MnO_2 in some levels, however, it was not conclusively and obviously demonstrated until microscopic analysis was applied to such

systems. Toupin et al., used *ex-situ* X-ray photoelectron spectroscopy (XPS) to determine the valence change of Mn during the redox process, in which Mn 3s and O 1s were used to characterize the valence change [24]. The energy separation between the two peaks of the Mn3s doublet (ΔE_b) shows an inverse linear relationship with the manganese oxidation state, and thus can be used as an probe of the MnO_2 redox process.

The augment and decrease in ΔE_b were observed during redox in a film electrode, which indicated the reversible variation of Mn valence. *In situ* X-ray absorption near-edge structure was used to give the direct evidence for variance of Mn valance [24]. In the same paper, a reversible expansion and shrinkage in lattice spacing of the oxide during charge transfer at manganese sites upon reduction/oxidation of MnO_2 was also demonstrated by *in-situ* synchrotron X-ray diffraction. A similar result was also obtained for a layered MnO_2. An increase of the interlayer spacing from 0.70 to 0.72 nm upon electrochemical oxidation indicated that alkaline metal cations, Na^+ ions, intercalated in the 2D tunnels of MnO_2 [25].

The facts of lattice expansion during redox process and a higher specific surface capacitance indicated that the insertion of cations in the electrolytes is predominating in the charge storage process of MnO_2. Meanwhile, an interesting result has obtained by Hu et al., [26]. They have synthesized single crystal of MnOOH, however, MnOOH is characterized to be inactive in the mild aqueous electrolyte, which means MnOOH is not the electroactive material responsible for the pseudo-capacitive reactions of MnO_2 in neutral media. Therefore, the charge storage mechanism of MnO_2 seems to be the tunnel storage of alkaline metal cations, expressed by equation 6.

As shown in Figure 1, there are various types of tunnel structures of MnO_2 and normally, these tunnels contain foreign cations. The tunnel structure properties of MnO_2 as well as foreign cations have also been investigated [22, 27, 28]. Various tunnel structures including 1D β (1×1), α (2×2), and γ (1×2), 2D δ (1×∞), and 3D λ structures.

The results showed that the small tunnel of β-MnO_2 was not suitable to store cations, while large tunnel size of α-MnO_2 favorites the storage of cations [22, 27]. In addition, the presence of other metal cations in the tunnel in advance, hinders the diffusion and storage of the electrolyte cations in the tunnel leading to a decrease in capacitance [28]. More recently, further researches on the tunnel storage of MnO_2 even revealed that the aprotic ionic liquids anions with the far bigger diameters than that of alkaline metal ion, such as DCA^- in butylmethyl pyrrolidinium-dicyanamide (BMP-DCA), could also be stored in the tunnels of MnO_2 [29]. Similar researches conducted that

thiocyanate (SCN$^-$) anion can reversibly insert/desert into/from the tunnels of MnO$_2$.
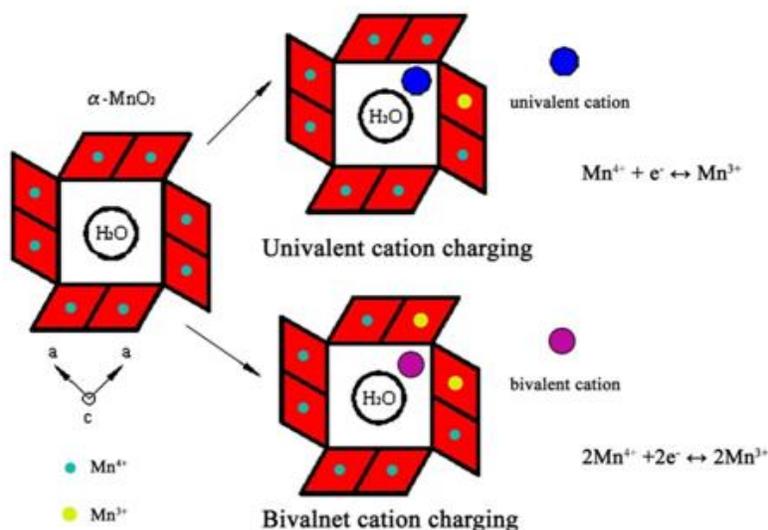

Figure 2. Comparison of univalent and bivalent cations intercalation process for multivalent cation storage mechanism [12, 31].

The reversible insertion process of aprotic anions with Mn^{3+}/Mn^{4+} transitions contributes to the ideal capacitive behavior of MnO$_2$ [30]. In such aprotic ionic liquids, the electrochemical potential window of MnO$_2$ has been enlarged to 3 V, three times higher than in the mild aqueous electrolytes, however, the stability of MnO$_2$ during cycling was not reported [29, 30].

Since the charge storage mechanism of MnO$_2$ involves the tunnel storage of cations and not only univalent alkaline metal cations, but bivalent cations such as alkaline-earth cations also usually present in the tunnels of MnO$_2$, more recently a multivalent cation storage mechanism has been proposed by Xu et al., [12, 31]. The realization of the theoretical capacity of a host material offered by its redox levels is determined by the number of intercalated ions concurrent with the charge transfer of the required number of electrons. From a vacancy point of view, multivalent cations may open up the possibility of electrodes, which exhibit higher gravimetric capacity and energy density. For example, we take univalent cation and bivalent cation intercalation process as samples. As shown in Figure 2, one univalent cation intercalated into the tunnel of α-MnO$_2$ only can force one Mn^{4+} ion to become Mn^{3+} ion and store one electron, but one bivalent cation can store two electrons, twice of that of

the univalent cation. In addition, the intercalation of polyvalent cations may be beneficial to the stability and reversibility of the host material because it demands fewer multivalent cations to achieve the same redox level. Therefore, it seems that the multivalent cation is advantageous of being used as the charge storage media because each multivalent cation can force multiple Mn^{4+} ions to become Mn^{3+} ion and store two electrons.

For the purpose of the multivalent cation storage mechanism, alkaline-earth metal cations (Mg^{2+}, Ca^{2+}, and Ba^{2+}) and trivalent cation (La^{3+}) are considered to be used as charge storage media to replace conventional alkaline cations (Li^+, Na^+, and K^+) [12, 31-35]. The results showed an ideal capacitive behavior of MnO_2 in the aqueous electrolytes containing these alkaline-earth metal cations. By replacing univalent cation with bivalent cation, for example, replacing conventional and widely used Na^+ ion with Ca^{2+} ion, a significant improvement on the specific capacitance of the same MnO_2 sample has been obtained [32, 34]. Ji et al., studied the effect of univalent and bivalent cations on electrochemical behaviors of MnO_2 with different crystallographic forms, which further confirmed that bivalent cation electrolytes leads to a relatively high specific capacitance value compared with univalentcation electrolytes and found that a progressive crystallinity loss of the material occurred upon cycling at the oxidized states [36]. One thing should be kept in mind that such improvement method is the most convenient and low cost.

4 ADVANCED MNO₂ MATERIALS AND ELECTRODES

Due to the variety in structures, MnO_2 can be synthesized in dozens of crystalline and disordered forms, each with unique physical properties, which is determined by the synthesis methods and procedures (for instant, heat treatment [23, 33, 37], washing by acid [22], or soaking in solution [38]) [39]. The physical properties in turn influence its electrochemical performance, which are highly relative to the electron conductivity and cations mobility.

Typically, there are two ways to utilize MnO_2 as supercapacitor electrode: the conventional composite electrode and thin film electrode architecture. In a common electrode for a mass application, MnO_2 powder, conductive additives, and a binder are blended, mixed with solutions to form a paste with a certain viscosity and then coated on a titanium or stainless steel current collector.

One of the most common methods to produce MnO_2 powder is co-precipitation method. The first paper related to the pseudo-capacitive behaviors of MnO_2 also adopted this easy method [9]. Generally, Mn (II) and

Mn (VII) sources are mixed together at certain concentration. Subsequently, the reaction begins and the nucleation and growth process occur. And after stirring for several hours, Mn (IV) precipitation will be produced.

$$3Mn(II) + 2Mn(VII) \rightarrow 5Mn(IV) \downarrow \qquad (7)$$

The Mn (IV) precipitation synthesized by this method without other process but baking at a low temperature (lower than 100 ℃) is normally amorphous α-MnO_2 with nearly 20% water. Its specific surface area could reach over 200 m^2 g^{-1} [40]. With a further heat treatment at several hundred degrees, the hydrous amorphous phase will dehydrate and transform into certain crystalline structure gradually. As a result, the crystalline grain increases and the specific surface area decreases, leading to the decrease in gravimetric capacitance and rate ability [41]. Based on the above reaction, various morphologies or crystalline structure of MnO_2 can be obtained by adjusting pH values [37, 42] and temperature [43, 44], adding additives [43, 45-48], changing Mn source, and using ultrasonic assistant [49, 50]. In addition, the strategies of replacing one of Mn source by acid or other agents(such as ethylene glycol [51], Cu [36] and so on) are also widely used to obtain MnO_2 [52-55].

Up to now, many other approaches to prepare MnO_2 powders have been gradually developed including sol-gel [19, 22, 56, 57], hydrothermal [58-63], molten salt route [64], thermal decomposition [65-67], solid state reaction[55, 68], sonochemical procedure [47, 49, 69, 70], microwave method [71-73], and so on. Various MnO_2 materials with different crystalline structures, morphologies, pore structures, and unique nanostructure architectures have been synthesized by changing the parameters or starting materials [72, 73]. Using the hydrothermal method as an example, Benhaddad et al., demonstrated that the structure, morphology and electrochemical reactivity of MnO_2 powders synthesized by using $(NH_4)_2S_2O_8$ are different from using $Na_2S_2O_8$ as oxidizing agent through the same hydrothermal process [74]. Later, Kalubarme et al., synthesized MnO_2 with needles, rods and flakes structure depending on another three oxidizers. The obtained MnO_2 flakes exhibit a specific capacitance of 342 F g^{-1} in NaOH electrolyte [75]. Li et al., reported that by changing the surfactant (polyvinylpyrrolidone, PVP) in the reacting solution, the correspondingly prepared MnO_2 showed varied morphology including ultralong nanowire, nanoflower and nanorod. Compared with MnO_2 nanorod, ultralong MnO_2 nanowire with a large aspect ratio exhibited a high conductivity, leading to a better electrochemical

property such as a specific capacitance of 345Fg^{-1} at a current density of 1Ag^{-1}. However only 88.1 F g^{-1} is measured for MnO_2 nanorod [76]. Zhu et al., synthesized MnO_2 nanostructures with controllable morphology by changing the reaction time or annealing process. Among all the morphology, MnO_2 nanotube structure assembled by nanosheets achieved an optimized electrochemical performance with an energy density of 13.33 kWkg^{-1} at a power density of 21.1 Whkg^{-1} [77]. Nayak et al., revealed that the morphologies and electrochemical performance of mesoporous MnO_2 materials changed with the hydrothermal temperature and reacting time. While they also found that through a rapid sonochemical synthesis process, the obtained MnO_2 materials is different from the MnO_2 materials synthesized by hydrothermal [70].

Although the specific capacitance of MnO_2 is affected by its physicochemical properties, for example, particle size, morphology, crystalline structure, etc., the resulting electrodes from MnO_2 powders generally deliver a specific capacitance lower than 250 F g^{-1} at a loading mass of a few mg cm^{-2} [22, 43, 45, 52, 69, 71, 72, 78-80]. And only when the loading mass decreased below 1 mg cm^{-2}, a few of samples can be reached a specific capacitance of 250 F g^{-1} [70]. The similar result occurs to micrometers-thick MnO_2 thin films, which was obtained by dip-coating, hydrothermal [59]), electrospinning [81], electrodeposition [82] or chemical bath deposition. Despite a capacitance of 450 F g^{-1} was reported by Nagarajan et al., [83], however, this high specific capacitance can only be obtained at a very low loading mass, less than 0.2 mg cm^{-2}. Moreover, only half of this value can be kept, if the loading mass increases to 0.3~0.4 mg cm^{-2} [17, 84-89]. Several groups have reported that when MnO_2 is formed as ultrathin films with loading mass lower than tens of μg cm^{-2} on metal current collector, anomalously high capacitances (over 1000 F g^{-1}) close to the theoretical values can be obtained [18, 24, 85]. A nanoscopically thin MnO_2 film significantly reduces the diffusion distances for the solid-state transport of insertion/extraction of cations and overcomes the limitations of the poor electronic conductivity of MnO_2 (10^{-5}~10^{-6} S cm^{-1}). However, due to extremely low loading mass, thin films seem to be limited to microsystems for energy storage such as integrated devices or to be used to analyze the charge storage mechanism. The weight of metal current collector for an industry application, such as Ni, Al, stainless steel, titanium foil, is normally a few mg cm^{-2}. Although the specific capacitance of ultrathin film is relatively high, however, if the loading mass of active materials is just one the hundred or one the thousands of current collector, the gravimetric or volumetric energy and power densities of MnO_2-based devices are

undoubtedly low. For anticipation to be used in a large scale, industrial application requires the use of the active material usually mixed with a binder and a conductive additive to prepare composite electrodes with a high loading mass or film electrode with improved thickness.

As the electrochemical storage process of MnO_2 involves the insertion of cations in the electrolytes or adsorption of ion on the surface, the decrease in solid-state diffusion distance of the electrolyte cations or increase in the specific surface area efficiently improve the utilization of MnO_2 at a fixed discharge or charge time. This advantage might fully exert at a high rate. Therefore, nanostructured MnO_2 with unique architecture and porous structure [51, 80, 90] is of great benefit to increasing electrolyte/electrode interface, shortening the distance of solid-state and aqueous transport of the electrolyte cations. And it continues to be the future trends in design and synthesis of MnO_2 materials. The unique architecture includes nanosphere with a few nanometers in diameter, ultrafine nanowire, ultrathin nanosheets, ultrasmall nanorod and nanoplate, etc. The hollow sphere, nanotube [76, 77, 91], or secondary nanostructure (such as nanoparticle [69, 81], tube [77], flower [72], even 3D structure [92] and so forth) [93] are also synthesized as new nanostructured materials.
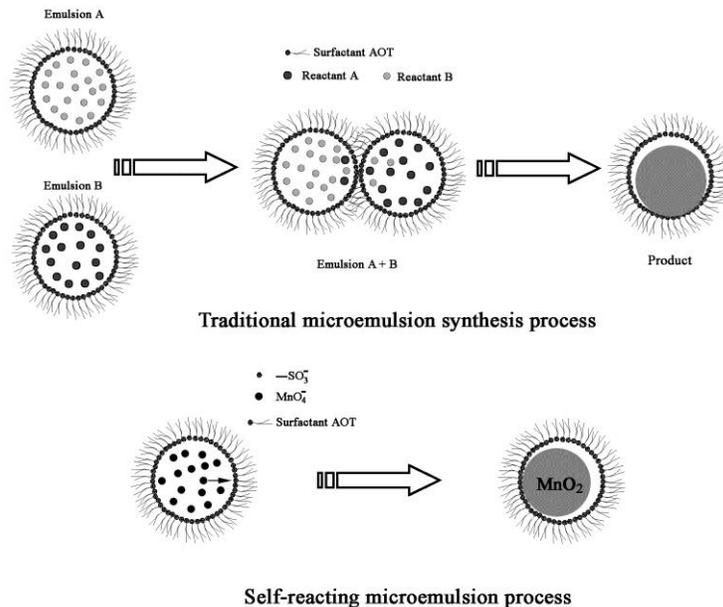

Figure 3. Synthesis process of traditional and self-reacting microemulsion [40].

Microemulsion is considered as a useful method to synthesize nanostructured particles with controllable size and morphologies, for example, nanosphere with a few nanometers in diameter, nanotube, nanowire, etc. [32, 47, 94-96].

Micro-nano droplets of water phase containing the reactants are dispersed and stabilized by a surfactant in an organic medium to form microemulsion. When the water pools (droplets) of two reactants collide, the reactants diffuse through surfactant layer between water pools. Therefore, the reactions carrying out in these droplets produce nanopaticles and the growth of the particles is restricted by surfactant when the particle size approaches to that of water pool, as shown in Figure 3. Devarj et al., utilized microemulsion to synthesize MnO_2 nanosphere with about 20 nm in diameter, its specific capacitance is 297 F g^{-1} [27]. C. Xu et al., proposed a self-reacting microemulsion process [40]. They noticed that $KMnO_4$, which is one of the most important raw materials to produce MnO_2, is a strong oxidation agent and can easily oxidize sulphonates to prepare manganese dioxide. On the other hand, one of the most common and low cost surfactants, sodium bis(2-ethylhexyl) sulfosuccinate (AOT) contains one sulphonate polar head group, which makes it capable of reducing $KMnO_4$. Therefore, a simple microemulsion was introduced to synthesize nanosized particles of manganese dioxides. The synthesis process of MnO_2 nanoparticles is shown in Figure 3. The reactant ($KMnO_4$) is firstly dispersed by AOT to form microemulsion automatically and then reduced by surfactant (AOT) without any other reluctant. This one step process can cut off the most of complicated and elaborated process. The reacting time can be compressed to half of an hour, while most of other methods need several hours or even days. The resulting particles possess nanosphere morphology with 4 nm in diameter. Due to enlarging the interface area of electrolyte/electrode and significantly shortening in solid-state transport distance of cations, a specific capacitance of 240 F g^{-1} was measured at a relative high loading mass. With the same procedure and raw materials, Xu et al., also prepared amorphous MnO_2 nanosheets (as thin as about 2 nm) with tunable size ranging from 5 nm to 20 nm [97]. The specific capacitance of ultrathin MnO_2 nanosheets is over 510 F g^{-1} at a scan rate of 2 mV s^{-1}, which is much higher than that of MnO_2 nanoparticles or nanorods. The results attribute to the lower thicknesses and high specific surface areas of the thin 2D nanosheets. The sheet morphology leadsto the direct contact of the sheet surface with the electrolyte and the short diffusion pathway of cations, which in turn gives a high capacitance even at a very high sweep rate and better capacitance retention rates. In addition, the physisorbed water and proton in the as-synthesized amorphous

MnO_2nanosheets to some extent facilitate the charge transfer and ions diffusion. The template method including hard and soft template is also one of the most important strategies to preparing various nanostructured as well as porous materials [98]. Tang et al., reported that MnO_2 hollow nanosphere was prepared through a templating-assisted hydrothermal process [62]. A SiO_2/MnO_2 core/shell nanosphere was firstly synthesized and the SiO_2 core was then removed by adding it into NaOH solutions. Finally MnO_2 hollow sphere with very thin wall was obtained, which delivers a high specific capacitance of about 300 F g^{-1} and good rate ability. With butyric acid as sacrificial template, Y. Munaiah et al., also successfully synthesized MnO_2 hollow sphere under ambient conditions for supercapacitor applications [32]. Mesoporous MnO_2 materials with various morphologies have also been frequently fabricated by using hard template [79, 99] as well as soft template. For instance, Nayak et al., prepared mesoporous MnO_2 nanoparticles and nanorods from $KMnO_4$ and poly(ethylene glycol)-block-poly(propylene glycol)-block-poly(ethylene glycol) (P123) acting as the soft template and reducing agent, which delivered a specific capacitance of 265 F g^{-1} at a current density of 1.0 A g^{-1}.
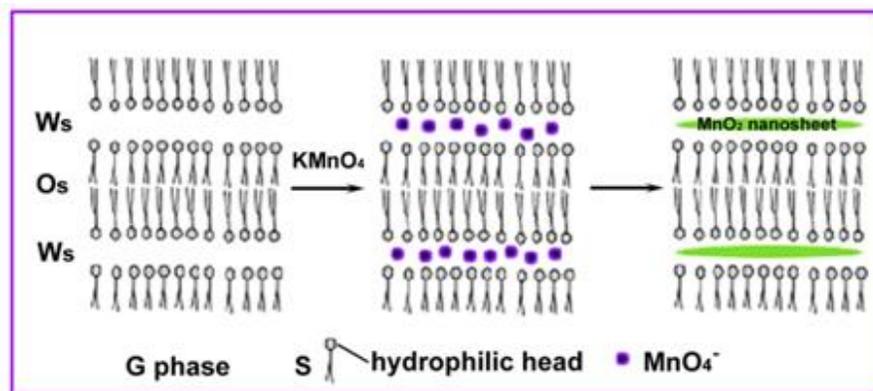

Figure 4. Schematic illustration of synthesis of MnO_2nanosheets. Os and Ws are organic and aqueous regions, respectively. S represents the surfactant AOT. The $KMnO_4$ is dissolved in the aqueous region and reduced by AOT to form MnO_2nanosheets.

With a soft template method, Shi et al., successfully synthesized well-dispersed ultrathin MnO_2 nanosheets (about 2 nm) by using $KMnO_4$ and AOT. At first, the AOT and water are mixed together. A unique lamellar structure is automatically formed as is showed in Figure 4, because the hydrophobic long

chain of surfactant tends to intertwine from each other to force hydrophilic heads toward the water phase in a binary phase. Then $KMnO_4$ is added in the solution and dissolved within the aqueous region. Finally, $KMnO_4$ is reduced by the hydrophilic head of AOT to produce MnO_2 and the growth of MnO_2 is restricted in the aqueous region by extra AOT, leading to the formation of MnO_2nanosheets.

Small-sized 0~2 D MnO_2 nanomaterials are terrifically unnecessary component during the formation of secondary nanostructured MnO_2. For instance, Li et al., and Xue et al., both fabricated MnO_2 fiber composed of 10 nm-scale MnO_2 particle through an electrospinning approach [81, 100]. Yuan et al., demonstrated that MnO_2 with a pillared-layer structure (or lamellar structure) caan be synthesized by an exfoliation/resembling and oxidation process [101].

Layered MnO_2 (birnissite phase) was firstly prepared and then treated in an aqueous solution of tetramethylammonium hydroxide for several days to obtain the slurry containing MnO_2 nanosheets [102, 103]. These nanosheets were restacked and oxidized to form lamellar MnO_2. Yan et al., reported that lamellar MnO_2 was synthesized by a hydrothermal route [104]. The lamellar structure is facile to the transport of the electrolyte cations and a high specific capacitance of 240 F g^{-1} was measured. MnO_2 powders with clew-like morphology composed of interleaving nanoplates as well as mesoporous characteristics were prepared by Wan et al., through a controlled crystal growth strategy.

The clew-like MnO_2 achieved a specific capacitance of 404.1 F g^{-1} in 1 mol L^{-1} Na_2SO_4 with loading mass of 10 mg cm^{-2}[105]. Likewise, Wang et al., reported that porous structured MnO_2 particles were assembled from ultrasmall MnO_2 nanorods (about 2 nm in diameter and 4~8 nm in length), which were synthesized from $KMnO_4$ and D-glucose in the presence of poly (ethylene glycol) by a facile sonochemistry procedure [69]. More recently, Yu et al., synthesized three-dimensional network mesoporous nanostructured MnO_2 from $KMnO_4$ and D-glucose system without using any surfactants [92]. The as-prepared MnO_2 powders showed a high capacitance of 283 F g^{-1} in $NaSO_4$ aqueous electrolyte and an enhanced rate capability compared with most of the other mesoporous α-MnO_2 in previous reports. Combined the simple, economic and large-scale synthesis strategy as well as the good overall electrochemical performance, MnO_2 powers synthesized with this template free method will show great potential for the practical supercapacitor applications.

However, the dynamics for energy storage in MnO_2 electrode includes not only cation mobility but also electron conductivity. The capacitance of MnO_2 powder electrodes with high mass loading or MnO_2 film electrodes with thick film will be ultimately limited by the poor electron conductivity of MnO_2 and weak contact with current collectors. The strategy of thin layer of MnO_2 directly coated or deposited on the current collector is used in MnO_2 film electrode. For example, short solid-state transport distance also have been translated to a nanostructured architecture of composite, in which MnO_2 deposits are incorporated with at least one kind of conductive materials including nanostructured carbon materials (for example, carbon black [106], activated carbon [107], porous carbon, graphitic carbon sphere [108, 109], carbon nanotube [106, 110-116], carbon nanofiber [117, 118], templated carbons [119], carbon aergel [120-122], grapheme [123-137], camphoric carbon nanobeads, etc. [109, 132, 137-140]), conducting polymer (such as polyaniline (PANI)[141-143], polypyrrole (Ppy) [144, 145], and poly (3,4-ethylenedioxythiophene) (PEDOT) [146, 147]), metal (Au particle or nanowire [148, 149], Ni foam [150], Mn nanotube[151], Te nanowire[152]), TiN[153], ITO nanowire, and so on [37, 108, 138, 142, 154-166]. For example, Reddy et al., reported Au-MnO_2/carbon nanotube hybrid coaxial arrays [167]. In such a structure, Au serves as the current collector and high surface area carbon nanotube array functions as supporter to improve the electron conductivity and utilization of MnO_2. The 3D structural design results in a very high power density.

Despite 3D MnO_2 based nanostructures are still being optimizing, the tentative results indicated a high utilization of MnO_2. More recently, some other materials, which can contribute capacitance or improve electrochemical behavior of MnO_2 electrodes like CoAl hydrotalcite, agarose gel, TiO_2, M(OH), CuO, NiO and $NiCo_2O_4$, are also gradually studied to hybrid with MnO_2 [168, 169].

In order to further improve the electrochemical behaviors of MnO_2, doping with other metal elements also has been attempted by researchers [170]. Kim et al., reported that the presence of other transition metal Ni or Pb in MnO_2 can improve the capacitance as well as the potential window of water decomposition [171]. Hereafter, Al, Co, Mo, V, and Fe have been considered to prepare binary oxides [167, 172-176]. The results showed that the substitution of alien metal species have a positive effect on the performance.

Experimentally, the physicochemical properties of MnO_2 materials are typically characterized with several measurements as follows. The versatile morphologies of MnO_2 are usually measured by using scanning electron

microscope (SEM) combined with transmission electron microscope (TEM). The surface topography and thickness of MnO_2 nanosheet can be visualized by atomic force microscopy (AFM) study. X-ray diffraction (XRD), Fourier transformation infrared (FTIR) spectra and Raman spectroscopy are frequently used to analyze the structure information of as prepared MnO_2. The Mn state and the composition of the synthesized MnO_2 can be further investigated by X-ray photoelectron spectroscopy (XPS) measurements.

5. ASYMMETRIC CAPACITORS BASED ON MnO₂

It is well known that the operating voltage of the aqueous symmetric supercapacitor (ASSP) is generally limited to about 1.0 V. For example, the principle performance limitation of an activated carbon ASSP is the narrow electrochemical potential window of the kinetics decomposition of water. The electrochemical potential window of a material is defined as the potential range or width, in which only capacitive behavior of this material takes place without any other irreversible redox reactions [177, 178]. The maximum cut-off voltage for MnO_2 is limited by the oxygen evolution or the oxidation process of Mn (IV) to Mn (VII). Meanwhile, the minimum cut-off voltage is determined by the reduction of Mn (III) to Mn (II) [179]. The solubility of Mn (VII) and Mn (II) species removes active material at each cycle of the electrode and the oxygen evolution adds irreversible redox process to the pseudo-capacitive process. The presence of oxygen may lead to the volumetric expansion and safety issues of supercapacitor. The capacitive electrochemical potential window of MnO_2 is normally 1.0 V, therefore, the cell voltage of a MnO_2 ASSP hardly exceeds 1.0 V. The low operating voltage limits MnO_2 ASSP to reach a high power or energy density.

In order to overcome the limited voltage window, one effective strategy is to design asymmetric supercapacitors, in which MnO_2 or its composite with a relatively high stable potential is only used as the positive electrode and a different electrode material with a relatively lower potential is served as the negative electrode. This smart design combines two different electrode materials with different electrochemical potential windows in a same cell. The difference between the upper cut-off potential of MnO_2 and the lower cut-off potential of negative electrode in a same electrolyte leads to an operating voltage higher than 1.0 V. The only one condition to design a MnO_2-based asymmetric capacitor is that the electrochemical potential window of other

electrode materials used as the negative electrode should be different from that of MnO_2.

In 2002, Hong et al., initially considered activated carbon (AC), which has been widely used as electrode material of EDLC, as the negative electrode material for MnO_2-based ASSP. They carefully noticed that both MnO_2 (standard amorphous α-MnO_2) and activated carbon (AC) show capacitive behavior in the same KCl electrolyte, but their capacitor potential windows are quite different. Subsequently, an asymmetric AC/MnO_2 supercapacitor was designed, in which the pseudo-capacitive storage mechanism of MnO_2 and the electric double layer storage mechanism of AC have been integrated in a same cell. The electrochemical characterizations indicated that the operating voltage of such an asymmetric supercapacitor can reach to 2.0 V, twice of that of ASSP. A relatively high energy density compared to RuO_2-based supercapacitor and organic EDLC was measured. Theoretically, to achieve a specific operating voltage of ASSP, the optimal mass ratio between MnO_2 and AC should be designed close to a theoretical value based on charge balance theory, their respective specific capacitances and potential window. The potential window of both MnO_2 and AC is sensitive to the electrolyte pH value. As the pH value is far from neutral, the potential difference between the upper cut-off potential of MnO_2 and the lower cut-off potential of hydrogen evolution of activated carbon varies [180]. It has also been demonstrated by Khomenko et al., who studied the influence of pH valve ranging from 6.4 to 10 and found the largest theoretical cell voltage of asymmetric AC/MnO_2 supercapacitor at pH$\approx$6.4. Except of AC, other form of carbon materials (such as Maxsorb [90], graphitic carbon sphere [139], carbon nanotube [181], carbon nanofiber [122, 181], grapheme [46], graphene hydrogel [129, 133] and so on) has also been intensively used as negative materials in carbon/MnO_2 asymmetric supercapacitor. Cao et al., reported that MnO_2/graphene asymmetric supercapacitor achieved an energy density of about 25.2Wh kg^{-1} at a power density of 100 W kg^{-1} in 1mol L^{-1} Na_2SO_4 aqueous electrolyte and exhibited good cycling performance (a capacitance retention of 96% even after 500 cycles).

A faradic or pseudo-capacitive electrode could also be used as the negative electrode together with a pseudo-capacitive MnO_2 electrode to build up an asymmetric supercapacitor. Metal oxide (Fe_3O_4, In_2O_3, MoO_3, etc.), conducting polymer or the composites are mainly chosen as the active material for negative electrode fabrication. For example, Fe_3O_4 as the low cost and environmentally friendly negative electrode has been proposed. The operating voltage of the Fe_3O_4/MnO_2 could reach to 1.8 V. However, the relative low

capacitance of Fe_3O_4 limited the asymmetric supercapacitor to achieve a high energy density [182].

Subsequently, $LiTi_2(PO_4)_3$ with a very high capacitance has been used as the negative electrode and a $LiTi_2(PO_4)_3/MnO_2$ asymmetric supercapacitor with maximum operating voltage of 1.9 V was built up [183]. As one kind of the most popular and important electrode materials, conducting polymer (such as polyaniline (PANI), polypyrrole (Ppy), and poly (3,4-ethylenedioxythiophene) (PEDOT)) have widely been considered as the negative electrodes together with MnO_2 to design asymmetric supercapacitor, whose operating voltages all reach to over 1.2 V [184]. Furthermore, composites based no less than one of mention-above negative electrode materials have also been used in MnO_2 based asymmetric supercapacitors. For example, $CNT@PANI$, $CNT@In_2O_3$, $Graphene@MoO_3$ composites materials have already been chosen as negative electrode materials in literature.

Combining a positive MnO_2 electrode with all the above-mentioned negative electrodes produces an increase of the cell voltage from about 1.0 V for the symmetrical supercapacitor up to 2.2 V for an AC/MnO_2 asymmetric device. As the energy density is proportional to the square of voltage and power density shows linear relationship with voltage, the performance of asymmetric supercapacitors in terms of power and energy densities can be significantly improved.

Except the effort to find new negative electrodes, the new forms of MnO_2 instead of amorphous MnO_2 have been attempted to be used as new positive electrode materials. Lamellar $NaMnO_2$ [185], $KMnO_2$ [186, 187] and spinel $LiMn_2O_4$ [188, 189] have been coupled with activated carbon to assemble the asymmetric supercapacitors. These capacitors showed promising performance. Moreover, it's reported that Lin et al., fabricated aqueous asymmetric supercapacitor with $MnFe_2O_4$ and $LiMn_2O_4$ as negative electrode and positive electrode, respectively. An energy density of about 10 Wh kg^{-1} was measured based on total mass of the two electrodes [188]. Interestingly, Yeager et al., fabricated $K_{0.15}MnO_2$ based asymmetric supercapacitors with a voltage of 1.2V, exhibiting an energy density of 15.4 and 10.7 Wh kg^{-1} using the PEDOT as its negative and positive electrode, respectively [187].

For above MnO_2-based asymmetric supercapacitors, the alkaline cations (Li^+, Na^+, or K^+) are widely used as the charge storage media. As shown in above section, by replacing univalent alkaline metal cations with multivalent cations as charge storage media, the specific capacitance of MnO_2 can be improved significantly.

Therefore, if these cations can be used in the asymmetric capacitors, the performance of asymmetric supercapacitor in terms of energy and power densities could be further increased. For example, the cycle voltammetry curves of activated carbon and MnO_2 in the aqueous electrolyte containing Ca^{2+} ions are shown in Figure 5. It is shown that the electrochemical potential window of MnO_2 is located between 0.1 and 1.0 V vs. saturated calomel electrode (SCE). Meanwhile, the potential range of AC could be controlled from −1.0 V to 0.1 V vs. SCE. Therefore, an asymmetric supercapacitor with 2.0 V operating voltage can be designed. The same results were also obtained for other alkaline metal cations (Ba^{2+} and Mg^{2+} ions) as well as trivalent La^{3+}ion.
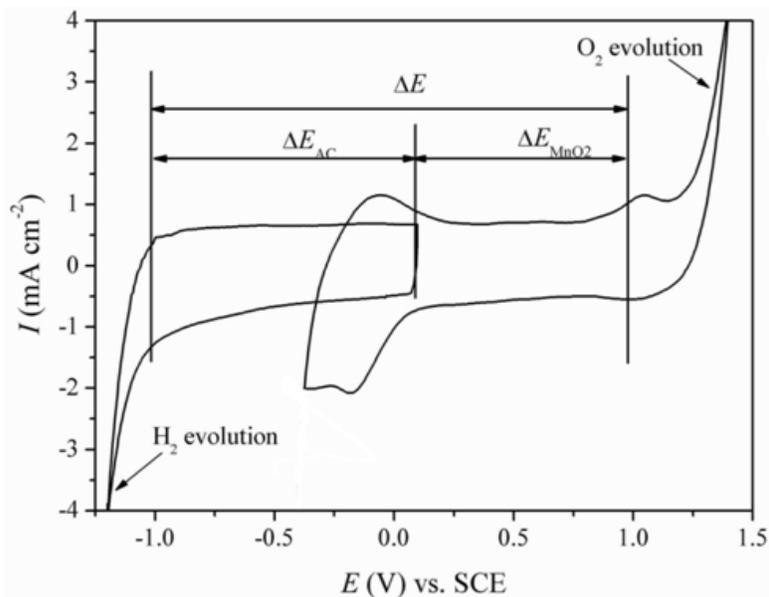

Figure 5. Cell operating potential range using 0.1 mol L^{-1} $Ca(NO_3)_2$ electrolytes [35].

Combined asymmetric design with the improved specific capacitance of the positive electrode due to the usage of the multivalent cations, the good performance of these asymmetric devices was reported [35]. To prevent the leakage, evaporation and corrosion of liquid electrolytes, and enhance the safety and reliability of the device, all-solid or gel-type electrolytes are gradually explored to be used into asymmetric supercapacitor [100, 165]. Generally, they are a mixture of a gel agent, a solute and a solvent. For example, the polyvinyl alcohol (PVA)/H_3PO_4 or PVA/H_2SO_4 electrolyte is

synthesized by firstly dissolving PVA gel agent into water and then adding H_3PO_4 or H_2SO_4 in the PVA/water solution. The solid electrolyte shows great potential in future transparent, flexible energy storage devices due to its safety and with no need of a separator had been used in fabricating solid-state flexible supercapacitor. Nam et al., reported that MnO_2 nanowire (with a mass loading of 1.02 mg cm^{-2} in electrode) exhibited a high specific capacitance of 484 F g^{-1} in potassium polyacrylate (PAAK)-based gel polymer electrolyte. Yu et al., reported that doping a redox mediator (for example p-phenylenediamine) into KOH electrolyte can significantly improve both the capacitance and cycling performance of MnO_2 symmetric supercapacitor. This simple and high-efficient redox-active electrolyte is believed to be a promising electrolyte in high-energy-storage asymmetric supercapacitor [190].

6. FLEXIBLE MnO_2 BASED SUPERCAPACITORS

Recently, the boost of wearable and bendable consumer electronics stimulates the development of advanced energy storage devices that not only have excellent electrochemical performance but also, more importantly, flexibility [191-195]. Compared with conventional supercapacitors, which are typically assembled by outer packages, current collectors (metal foil), positive/negative electrodes, electrolyte, and separator (Figure 6a). The structure of flexible supercapacitors is simplified with no need of independent current collectors (Figure 6b) and free of binders, because the above-mentioned carbon networks in flexible electrodes with high conductivity and flexibility usually act as current collectors that substitute for metal foils. Some soft and bendable plastic (such as polybag, ethylene/vinylacetatecopolymer (EVA) film, polyethyleneterephthalate (PET), PDMS and telfon substrate) has been widely used as the package leading to fully flexible supercapacitor [191]. The simplified architecture is bendable, flexible and light-weight compared with conventional supercapacitor.

Asymmetric supercapacitors based on flexible MnO_2 electrodes to achieve both high energy densities and flexibility have been studied and reported intensively. Firstly, flexible MnO_2 electrodes are fabricated with the flexible conducting substrate (such as most commonly used carbon networks [116, 196-203], indium tin oxide film [204], metal [205, 206] and so on) as main infrastructure to reserve the flexibility. MnO_2 or its composites are coated onto flexible conducting infrastructure through a variety of methods such as electro-deposition, chemical deposition, printing method, *in situ* growth, etc., [191].

For example, MnO_2 with various morphology was electro deposited onto carbon fabricate an adequate current density in an aqueous solution (such as Mn $(CH_3COO)_2$+CH_3COONH_4,H_2SO_4+$MnSO_4$, and so on) followed by washing with deionized water [197, 199, 203]. Mostly, the thickness or loading mass of MnO_2 can be controlled by some parameters for instance the deposit time. Chenetal used MnO_2@ carbon composite manufactured highly flexible supercapacitors with a specific capacitance of 425 F g^{-1}. Luetal reported that flexible WO_{3-x}@Au@MnO_2 electrodes exhibited an outstanding electro chemical performance (a specific capacitance of 588Fg^{-1}atascanrate of 10 mV s^{-1} and 1195F g^{-1}at 0.75 A g^{-1}), where the energy density can reach 106.4 Wh kg^{-1} at a power density of 23.6 kW kg^{-1}[201].
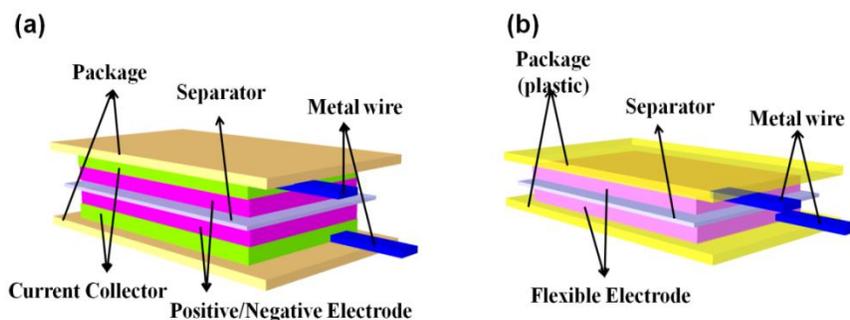

Figure 6. Schematic illustration of a traditional (a) and flexible (b) supercapacitor [191].

Shi et al., recently reported a simple screen-printing strategy to fabricate flexible electrodes as well as flexible supercapacitor [204]. This method is also available to almost any other electrode materials without the assistant of carbon networks. The screen-printing processes of supercapacitor are presented in Figure 7. Before printing, it is necessary to prepare the three key elements known as printing ink, screen plate and printing stock. The ink is prepared by dispersing powders of electrode material in water or organic solvents. Occasionally, binders and conductive additives are added to enhance the adhesivity and conductivity when necessary.

Shi et al., prepared the aqueous printing inks of manganese dioxide nanosheets prepared with above mentioned soft template method and grapheme aerogel powders, respectively. With a screen plate containing blind-holes and through-holes, the ink is printed on the printing stock through the through-holes. The through-holes can be designed as various patterns, pictures or letters, such as a cute "panda", "Tsinghua University" letters and star-

shaped or dot patterns [204]. This character leads to its critical role, like "the magic paint brush", in creating various vivid supercapacitors such as a "panda" supercapacitor. The printing stock can be soft paper, cloth, plastic, hard glass, ceramic, etc. As an example, a flexible and transparent indium tin oxide/polyethylene terephthalate (ITO-PET) plate is used as printing stock which functions as both current collector and outer package of the supercapacitor by Shi et al. The structure of ITO-PET is one face of a PET plate (thickness is about 0.125 mm) uniformly coated by a thin ITO film (sheet resistance is 40 Ω sq^{-1}). The ITO layer serves as the current collector, while PET plate functions as flexible outer package. Owing to the high conductivity of flexible ITO-PET substrate, it can substitute for the outer package, metal current collector and metal lead wire used in traditional supercapacitor leading to a simplified architecture of the flexible supercapacitor. The screen-printed supercapacitor was fabricated by two electrodes sandwiched with $Ca(NO_3)_2$-SiO_2 composite gel electrolyte. It has to be pointed out that this screen printing method is suitable for inks made of almost all electrode materials in kinds of solvents, and the printing stock can be soft, hard, flat, curved as well as various shape and size.
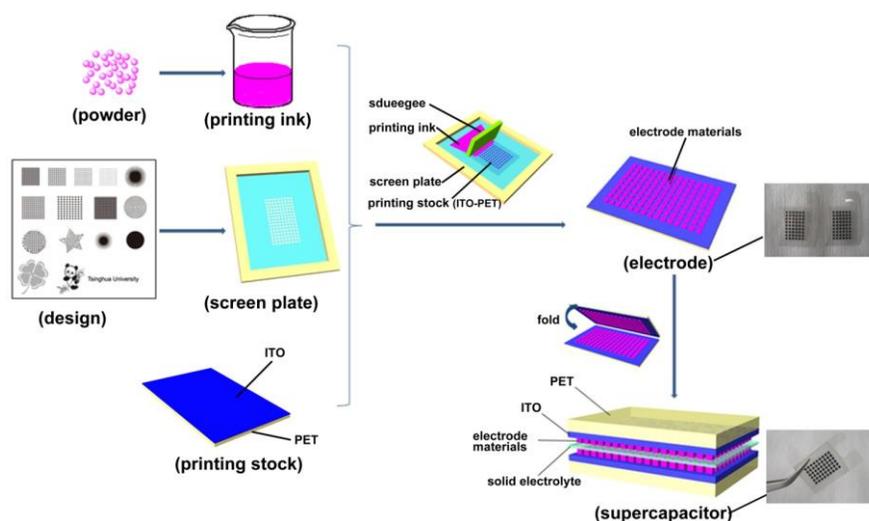

Figure 7. Schematic illustration of the fabrication of screen-printed supercapacitors. Firstly, the ink is printed on the printing stock through screen plate to prepare the flexible electrode with certain patterns. Then the two identical or different flexible electrodes with electrolyte are assembled to be symmetric or asymmetric supercapacitor [204].
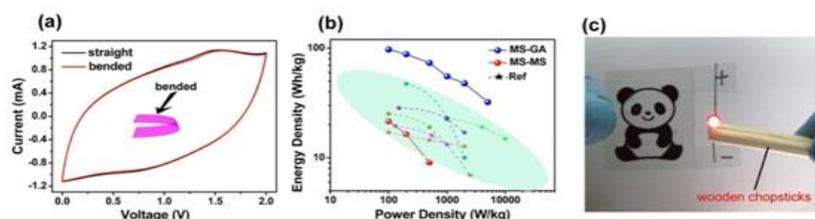
Figure 8. Evaluation of the performance of screen-printed supercapacitors. (a) Cyclic voltammetry (CV) curves of straight and bended supercapacitor at a scan rate of 20 mV s^{-1}. (b) Ragone plots of MS/GA and MS/MS supercapacitor compared with other MnO_2 based asymmetric supercapacitors in literature (based on the total mass of active materials). Here, MS refers to MnO_2 nanosheets and GA refers to graphene aerogel nanosheets. (c) Photograph of the "panda" asymmetric MS/GA supercapacitor lighting up a red light emitting diode (LED).

In addition, electrode materials printed on the ITO layer with especially beautiful contact are thickness-controllable and stable. Most interestingly, the versatile tool of "screenplate" provides the electrodes or supercapacitors preferred transparency and pattern. The screen-printed supercapacitor is not only an excellent energy storage device with flexibility but also an artwork. As is showed in Figure 8a, it can be seen that cyclic voltammetry (CV) curves of supercapacitor before and after being bended show almost the same. This result clearly shows the good flexibility of the screen-printed supercapacitor. Asymmtric supercapacitors based on two dimensional ultrathin MnO_2 and grapheme nanosheets realized excellent electro chemical performance such as a high energy density of 97.2 Wh kg^{-1} (Figure 8b). What's more, an asymmetric supercapacitor with a vivid "panda" pattern was manufactured for the first time by Shi et al. The panda supercapacitor has a voltage of 2.0 V capable of lighting up a red light emitting diode as shown in Figure 8c. It indicates another, quite different aspect that a battery or supercapacitor is no longer a cold industry product, but could have the meaning of art. Table 1 gives a summary of the performance of the asymmetric supercapacitors including flexible ones based on MnO_2 or its composites, briefly. The expanded voltage range as well as the improvement on the performance of positive and negative electrodes enables the energy density of asymmetric supercapacitors reach to above 20 Wh Kg^{-1} (based on the active material mass of both electrodes), nearly one order of aqueous symmetric capacitor and even higher than organic AC symmetric capacitors. It means that MnO_2-based asymmetric supercapacitors show great potential to be used in mass applications, open the new way for low cost manufacturing of high-energy devices.

Table 1. The summarized data of MnO$_2$ based supercapacitors from literatures

Negative electrode	Positive electrode	Electrolyte salt	Voltage (V)	Capacitance (F g^{-1})	Power density (KW Kg^{-1})	Energy density (Wh Kg^{-1})	Cycle numbers	Ref.
AC	MnO$_2$	KCl	2.0	52	0.5	28.8	100	[10]
AC	MnO$_2$	K$_2$SO$_4$	2.2	31	3.6	10	10,000	[207]
AC	MnO$_2$	K$_2$SO$_4$	1.5	-	10	7.0	23,000	[207]
AC	MnO$_2$	K$_2$SO$_4$	2.0	21	- 10	11.7 10	195,000	[208]
AC	MnO$_2$	K$_2$SO$_4$	1.8	-	2.0, 0.15	17, 28.4	23 000	[209]
AC	MnO$_2$	K$_2$SO$_4$	1.5	30.0mF m^{-2}	0.4 W cm^{-3}	9.0mWhcm^{-3}		[210]
AC	MnO$_2$	KNO$_3$	2.0	140	0.123	21.0	1000	[211]
AC	MnO$_2$	Na$_2$SO$_4$	2.0	30.8	0.1, 2.0	17.1, 12.7		[93]
AC	MnO$_2$	Na$_2$SO$_4$	1.8	46.5	0.1, 1.7	20.9, 12.5	10,000	[212]
AC	MnO$_2$	Ca(NO$_3$)$_2$	2.0	37	0.3	21	5,000	[35]
AC	MnO$_2$	[Bmim]PF$_6$/DMF	3.0	-	0.59, 20.4	67.5, 8.5	--	[213]
RGO	MnO$_2$	Na$_2$SO$_4$	2.0	37	0.1	25.2	500	[46]
RGO	MnO$_2$	Na$_2$SO$_4$	2.0	41.7	1.0, 10	23.2, 14.9	5000	[129]
Maxsorb	MnO$_2$	Na$_2$SO$_4$	1.7	81.5			2000	[90]
CNT-CNF	MnO$_2$	Na$_2$SO$_4$	2.0	94, 55.3	0.1, 1.0	52.2, 30.7	2000	[181]
AC	K$_{0.27}$MnO$_2$·0.6H$_2$O	K$_2$SO$_4$	1.8	-	0.14, 2.0	25, 17.6	10000	[186]
AC	NaMnO$_2$	Na$_2$SO$_4$	1.8	-	0.13	19.5	-	[185]
AC	LiMn$_2$O$_4$	Li$_2$SO$_4$	1.8	-	0.1, 2.0	35, 10	20,000	[189]

Negative electrode	Positive electrode	Electrolyte salt	Voltage (V)	Capacitance (F g^{-1})	Power density (KW Kg^{-1})	Energy density (Wh Kg^{-1})	Cycle numbers	Ref.
PANI	MnO_2	KNO_3	1.2	-	42.1	5.9	500	[184]
Ppy	MnO_2	KNO_3	1.4	-	62.8	7.4	500	[184]
PEDOT	MnO_2	KNO_3	1.8	-	120.1	13.5	500	[184]
Fe_3O_4	MnO_2	K_2SO_4	1.8	20	0.82	7.0		[182]
$LiTi_2(PO_4)_3$	MnO_2	Li_2SO_4	1.9	-	0.2	47	1000	[183]
$MnFe_2O_4$	$LiMn_2O_4$	$LiNO_3$	1.3	-	0.3, 1.8	10, 5.5	5000	[188]
AC	MnO_2/AC	Na_2SO_4	2.0	50.6		28.1	1000	[107]
AC	MnO_2/AC	Na_2SO_4	1.8	22.1	-	-	1500	[51]
AC	MnO_2/CNT	Na_2SO_4	2.0	55.7	0.2, 20.8	30.6, 8.7	5000	[122]
RGO	MnO_2/ RGO	Na_2SO_4	1.8	53	0.225	23.9	1000	[132]
RGO	MnO_2/ RGO	Na_2SO_4	1.8	0.89Fcm^{-2}	-	0.72mWh cm^{-3}	10 000	[133]
RGO	MnO_2/Ni(OH)$_2$	KOH	1.6	538	0.78, 8.67	186, 42.5	3000	[214]
RGO/MoO$_3$	MnO_2/RGO	Na_2SO_4	2.0	307	0.27	42.6	1000	[215]
GCS	MnO_2/GCS	Na_2SO_4	2.0	190	7.0	22.1	1000	[139]
N-Doped CNT	MnO_2/CNF	Na_2SO_4	2.0	-	~0.2, 284.6	32.9, <10	2000	[216]
Flexible								
CNT	MnO_2/RGO	Na_2SO_4	1.5	-	110	12.5	5000	[202]
CNF	MnO_2/RGO	polymer	>3.0	-	-	-	-	[217]
AC	MnO_2/PEDOT	Na_2SO_4	2.0	-	0.38W cm^{-3}	0.36 mWhcm^{-3}	-	[205]
In$_2$O$_3$/CNT	MnO_2/CNT	Na_2SO_4	2.0	184	50.3	25.5	-	[218]
RGO/Ag	MnO_2/RGO	Na_2SO_4	1.8	112.8	0.1, 90.3	50.8, 7.53	-	[219]
CNT/PANI	CNT/MnO_2/RGO	Na_2SO_4/PVP	1.6	-	~ 0.2	24.8	-	[220]

Note: graphitic carbon sphere donates as GCS, graphene, graphene foam, or reduced graphene and donate as RGO, carbon nanofiber donates as CNF.

7. OPPORTUNITIES AND CHALLENGES IN FUTURE

Aqueous MnO_2-basedasymmetriccapacitors show the advantages in device manufacturing: low-cost and environmentally friendly materials and components, no need for moisture-free atmospheres during cell assembly, and the use of simple nontoxic salts and electrolytes. In addition, the superiority of the aqueous device was also characterized with higher thermal safety because of the vaporization temperature and non-flammability of the aqueous electrolyte.

It is worth to notice that the advantages of widely used Zn/MnO_2 batteries, approximate 60 billion pieces per year, are based on the facts that the cost of all components, especially MnO_2 and Zn, and manufacturing fee are totally low. Therefore, MnO_2 based supercapacitors are anticipated to be applied in mass applications.

It is well known that the theoretical value of specific capacitance of MnO_2 is about $1380 Fg^{-1}$. In order to further improve the performance of MnO_2-based supercapacitor for mass applications, MnO_2 materials is necessary to be design into nanoarchitectures or composites with other materials, such as porous carbon or polymer. Since the biggest advantage of MnO_2 is its low cost and abundance in resource, new synthesis methods with low cost and simple process are vital important for final commercialization. The electrolyte is also an important factor for MnO_2-basedsystems. Recently, a gel-type electrolyte has been tentatively applied in MnO_2-based systems [221]. The gel electrolyte will prevent leaking of the electrolyte, which is superior to a liquid electrolyte. Although the manufacturing cost of such gel-type device will undoubtedly be high, it will open up a new direction to develop reliable MnO_2-based devices.

Although the intercalation redox process of the electrolyte cations (alkaline metal cations or alkaline-earth metal cations) is predominate in the charge storage mechanism of MnO_2, there are still anomalous phenomena that the specific capacitance of MnO_2 will increase with increase in pH values of the electrolytes and the adsorbed water or hydrous species also play an important role in the charge process [50]. Therefore, the charge storage mechanism of MnO_2 should be clarified in more details, for example, the effect of protons and physically or chemically adsorbed water, and the influence of physicochemical properties such as particle size, crystalline structures, water content, specific surface area, or surface state, and so on. A detailed knowledge of the charge storage mechanism of MnO_2 is of the vital importance to further control factors that govern the charge-storage process

and to develop materials and electrode structures with improved electrochemical performance.

The advantages of improved MnO_2 electrode and increased cell voltage for MnO_2 based supercapacitors, must be incorporated with the total optimization of other components, such as continuous search of pertinent complementary negative electrode with good electrochemical performance, or weight balance between the positive and negative electrodes. The irreversible reactions for instance, dissolution of manganese, evolution of hydrogen and oxygen, or other non-capacitive behavior of negative electrode, limit the cycle performance of MnO_2. The requirement for the commercial supercapacitors is more than 100,000 cycles. Therefore, the potentials of both electrodes have to be carefully monitored in order to avoid capacity fade upon cycling. For AC/MnO_2 asymmetric devices, it would be not the problem, because the stability of AC electrode is a less critical issue and up to nearly two hundreds of thousands cycles have been reported for such devices [208]. However, for a pseudo-capacitive or faradic negative electrode, it is necessary to be more careful, since only 100 to 1000 cycles was reported in such systems. In addition, the technologies involving in the integral devices are also ultimately important for final mass applications. The continuous production and assembly of electrode and the integral devices have to be built up and optimized.

REFERENCES

[1]   Burke, A., Ultracapacitors: why, how, and where is the technology. *Journal of Power Sources*, 2000. 91(1): p. 37-50.

[2]   Yoda, S. and K. Ishihara, The advent of battery-based societies and the global environment in the 21st century. *Journal of Power Sources*, 1999. 81: p. 162-169.

[3]   Conway, B.E., *Electrochemical Supercapacitor: Scientific Fundamentals and Technological Applications.* Kluwer Academic /Plenum Publishers, New York, 1999.

[4]   Yoshino, A., et al., Development of a lithium-type advanced energy storage device. *Journal of The Electrochemical Society*, 2004. 151(12): p. A2180-A2182.

[5]   Becker, H., An electrochemical capacitor. *U.S. Patent* No.2800616[P], 1957.

[6]   Zheng, J.P., Ruthenium oxide-carbon composite electrodes for electrochemical capacitors. *Electrochemical and Solid State Letters,* 1999. 2(8): p. 359-361.

[7]   Zheng, J.P., P.J. Cygan, and T.R. Jow, Hydrous Ruthenium Oxide as an Electrode Material for Electrochemical Capacitors. *Journal of The Electrochemical Society,* 1995. 142(8): p. 2699-2703.

[8]   Lee, H.Y. and J.B. Goodenough, Ideal supercapacitor behavior of amorphous V2O5 center dot nH(2)O in potassium chloride (KCl) aqueous solution. *Journal of Solid State Chemistry*, 1999. 148(1): p. 81-84.

[9]   Lee, H.Y. and J.B. Goodenough, Supercapacitor behavior with KCl electrolyte. *Journal of Solid State Chemistry*, 1999. 144(1): p. 220-223.

[10]   Hong, M.S., S.H. Lee, and S.W. Kim, Use of KCl aqueous electrolyte for 2 V manganese oxide/activated carbon hybrid capacitor. *Electrochemical and Solid State Letters*, 2002. 5(10): p. A227-A230.

[11]   Belanger, D., T. Brousse, and J.W. Long, Manganese oxides: battery materials make the leap to electrochemical capacitors. *Electrochemical Society Interface,* 2008. 17(1): p. 49-52.

[12]   Xu, C., et al., Capacitive Behavior and Charge Storage Mechanism of Manganese Dioxide in Aqueous Solution Containing Bivalent Cations. *Journal of The Electrochemical Society*, 2009. 156(1): p. A73-A78.

[13]   Handbook of battery materials. *Handbook of battery materials,* ed. J.O. Besenhard1999. 636 pp-636 pp.

[14]   Machefaux, E., et al., Supercapacitor behavior of new substituted manganese dioxides. *Journal of Power Sources*, 2007. 165(2): p. 651-655.

[15]   Lee, M.-T., et al., Annealed Mn-Fe binary oxides for supercapacitor applications. Journal of Power Sources, 2008. 185(2): p. 1550-1556.

[16]   Trasatti, S., Physical Electrochemistry of Ceramic Oxides. *Electrochimica Acta*, 1991. 36(2): p. 225-241.

[17]   Hu, C.C. and T.W. Tsou, Ideal capacitive behavior of hydrous manganese oxide prepared by anodic deposition. Electrochemistry *Communications,* 2002. 4(2): p. 105-109.

[18]   Pang, S.C., M.A. Anderson, and T.W. Chapman, Novel electrode materials for thin-film ultracapacitors: Comparison of electrochemical properties of sol-gel-derived and electrodeposited manganese dioxide. *Journal of The Electrochemical Society*, 2000. 147(2): p. 444-450.

[19] Reddy, R.N. and R.G. Reddy, Sol-gel MnO2 as an electrode material for electrochemical capacitors. *Journal of Power Sources*, 2003. 124(1): p. 330-337.

[20] Kadoma, Y., et al., Synthesis of hollandite-type LiMnO2 by Li+ ion-exchange in molten salt and lithium insertion characteristics. *Electrochimica Acta*, 2007. 53(4): p. 1697-1702.

[21] Johnson, C.S., Development and utility of manganese oxides as cathodes in lithium batteries. *Journal of Power Sources*, 2007. 165(2): p. 559-565.

[22] Brousse, T., et al., Crystalline MnO2 as possible alternatives to amorphous compounds in electrochemical supercapacitors. *Journal of The Electrochemical Society,* 2006. 153(12): p. A2171-A2180.

[23] Toupin, M., T. Brousse, and D. Belanger, Influence of microstucture on the charge storage properties of chemically synthesized manganese dioxide. *Chemistry of Materials*, 2002. 14(9): p. 3946-3952.

[24] Toupin, M., T. Brousse, and D. Belanger, Charge storage mechanism of MnO2 electrode used in aqueous electrochemical capacitor. *Chemistry of Materials,* 2004. 16(16): p. 3184-3190.

[25] Athouel, L., et al., Variation of the MnO2 birnessite structure upon charge/discharge in an electrochemical supercapacitor electrode in aqueous Na2SO4 electrolyte. *Journal of Physical Chemistry* C, 2008. 112(18): p. 7270-7277.

[26] Hu, C.-C., Y.-T. Wu, and K.-H. Chang, Low-temperature hydrothermal synthesis of Mn3O4 and MnOOH single crystals: Determinant influence of oxidants. *Chemistry of Materials*, 2008. 20(9): p. 2890-2894.

[27] Devaraj, S. and N. Munichandraiah, Effect of crystallographic structure of MnO2 on its electrochemical capacitance properties. *Journal of Physical Chemistry* C, 2008. 112(11): p. 4406-4417.

[28] Ghodbane, O., J.-L. Pascal, and F. Favier, Microstructural Effects on Charge-Storage Properties in MnO2-Based Electrochemical Supercapacitors. *ACS Appl. Mater. Interfaces*, 2009. 1(5): p. 1130-1139.

[29] Chang, J.-K., et al., X-ray Photoelectron Spectroscopy and in Situ X-ray Absorption Spectroscopy Studies on Reversible Insertion/Desertion of Dicyanamide Anions into/from Manganese Oxide in Ionic Liquid. *Chemistry of Materials*, 2009. 21(13): p. 2688-2695.

[30] Lee, M.-T., et al., Pseudocapacitance of MnO2 originates from reversible insertion/desertion of thiocyanate anions studied using in situ X-ray absorption spectroscopy in ionic liquid electrolyte. *Journal of Power Sources,* 2010. 195(3): p. 919-922.

[31] Xu, C., et al., Reversible Insertion Properties of Zinc Ion into Manganese Dioxide and Its Application for Energy Storage. *Electrochemical and Solid State Letters*, 2009. 12(4): p. A61-A65.

[32] Munaiah, Y., et al., Facile synthesis of hollow sphere amorphous MnO2: the formation mechanism, morphology and effect of a bivalent cation-containing electrolyte on its supercapacitive behavior. *Journal of Materials Chemistry A,* 2013. 1(13): p. 4300.

[33] Kumar Nayak, P. and N. Munichandraiah, Reversible Insertion of a Trivalent Cation onto MnO2 Leading to Enhanced Capacitance. *Journal of The Electrochemical Society,* 2011. 158(5): p. A585.

[34] Hu, C.-C., et al., A hierarchical nanostructure consisting of amorphous MnO2, Mn3O4 nanocrystallites, and single-crystalline MnOOH nanowires for supercapacitors. *Journal of Power Sources*, 2011. 196(2): p. 847-850.

[35] Xu, C., et al., Asymmetric Activated Carbon-Manganese Dioxide Capacitors in Mild Aqueous Electrolytes Containing Alkaline-Earth Cations. *Journal of The Electrochemical Society*, 2009. 156(6): p. A435-A441.

[36] Ji, C.-C., et al., Effect of alkaline and alkaline–earth cations on the supercapacitor performance of MnO2 with various crystallographic structures. *Journal of Solid State Electrochemistry*, 2013. 17(5): p. 1357-1368.

[37] Wei, C., et al., Anomalous effect of K ion on crystallinity and capacitance of the manganese dioxide. *Journal of Power Sources*, 2013. 225: p. 226-230.

[38] Aronson, B.J., et al., Synthesis, characterization, and electrochemical properties of magnesium birnessite and zinc chaclophanite prepared by a low-temperature route. *Chemistry of Materials*, 1999. 11(4): p. 949-957.

[39] Wei, W., et al., Manganese oxide-based materials as electrochemical supercapacitor electrodes. Chem Soc Rev, 2011. 40(3): p. 1697-721.

[40] Xu, C., et al., Electrochemical properties of nanosized hydrous manganese dioxide synthesized by a self-reacting microemulsion method. *Journal of Power Sources*, 2008. 180(1): p. 664-670.

[41] Devaraj, S., and N. Munichandraiah, Electrochemical supercapacitor studies of nanostructured a-MnO2 synthesized by microemulsion method and the effect of annealing. *Journal of The Electrochemical Society*, 2007. 154(2): p. A80-A88.

[42] Jeong, Y.U. and A. Manthiram, Nanocrystalline manganese oxides for electrochemical capacitors with neutral electrolytes. *Journal of The Electrochemical Society,* 2002. 149(11): p. A1419-A1422.

[43] Zhang, H., Y. Wang, and C. Wang, Influence of surfactant on the capacitive performance of manganese dioxide prepared at different temperatures. *Energy Conversion and Management*, 2013. 74: p. 286-292.

[44] Chen, S., et al., Shape-Controlled Synthesis of One-Dimensional MnO2 via a Facile Quick-Precipitation Procedure and its Electrochemical Properties. *Crystal Growth & Design*, 2009. 9(10): p. 4356-4361.

[45] Song, Z., et al., A facile template-free synthesis of α-MnO2 nanorods for supercapacitor. *Journal of Alloys and Compounds*, 2013. 560: p. 151-155.

[46] Cao, J., et al., High voltage asymmetric supercapacitor based on MnO2 and graphene electrodes. *Journal of Electroanalytical Chemistry*, 2013. 689: p. 201-206.

[47] Sumboja, A., et al., Monitoring electroactive ions at manganese dioxide pseudocapacitive electrodes with scanning electrochemical microscope for supercapacitor electrodes. *Journal of Power Sources*, 2012. 207: p. 205-211.

[48] Jiang, R., et al., A novel method to prepare nanostructured manganese dioxide and its electrochemical properties as a supercapacitor electrode. *Electrochimica Acta*, 2009. 54(11): p. 3047-3052.

[49] Nam, H.-S., et al., Electrochemical Capacitances of a Nanowire-Structured MnO2 in Polyacrylate-Based Gel Electrolytes. *Journal of The Electrochemical Society,* 2012. 159(6): p. A899.

[50] Ghaemi, M., et al., Charge storage mechanism of sonochemically prepared MnO2 as supercapacitor electrode: Effects of physisorbed water and proton conduction. *Electrochimica Acta*, 2008. 53(14): p. 4607-4614.

[51] Wang, Y.-T., A.-H. Lu, and W.-C. Li, Mesoporous manganese dioxide prepared under acidic conditions as high performance electrode material for hybrid supercapacitors. *Microporous and Mesoporous Materials,* 2012. 153: p. 247-253.

[52] Beaudrouet, E., A.L.G. La Salle, and D. Guyomard, Nanostructured manganese dioxides: Synthesis and properties as supercapacitor electrode materials. *Electrochimica Acta,* 2009. 54(4): p. 1240-1248.

[53] Luo, J.-Y., X.-L. Li, and Y.-Y. Xia, Synthesis of highly crystalline spinel LiMn2O4 by a soft chemical route and its electrochemical performance. *Electrochimica Acta,* 2007. 52(13): p. 4525-4531.

[54] Ni, J., et al., Low-Temperature Synthesis of Monodisperse 3D Manganese Oxide Nanoflowers and Their Pseudocapacitance Properties. *Journal of Physical Chemistry* C, 2009. 113(1): p. 54-60.

[55] Ragupathy, P., et al., Remarkable Capacity Retention of Nanostructured Manganese Oxide upon Cycling as an Electrode Material for Supercapacitor. *Journal of Physical Chemistry* C, 2009. 113(15): p. 6303-6309.

[56] Long, J.W., et al., Design of pore and matter architectures in manganese oxide charge-storage materials. *Electrochemical and Solid State Letters,* 2000. 3(10): p. 453-456.

[57] Franger, S., et al., Synthesis, structural and electrochemical characterizations of the sol-gel birnessite MnO1.84 center dot 0.6H(2)O. *Journal of Power Sources*, 2002. 109(2): p. 262-275.

[58] Yan, D., et al., MnO2 film with three-dimensional structure prepared by hydrothermal process for supercapacitor. *Journal of Power Sources,* 2012. 199: p. 409-412.

[59] Yao, W., et al., Flexible α-MnO2 paper formed by millimeter-long nanowires for supercapacitor electrodes. *Journal of Power Sources,* 2014. 247: p. 824-830.

[60] Subramanian, V., H. Zhu, and B. Wei, Nanostructured MnO2: Hydrothermal synthesis and electrochemical properties as a supercapacitor electrode material. *Journal of Power Sources*, 2006. 159(1): p. 361-364.

[61] Subramanian, V., et al., Hydrothermal synthesis and pseudocapacitance properties of MnO2 nanostructures. *Journal of Physical Chemistry B,* 2005. 109(43): p. 20207-20214.

[62] Tang, X., et al., Synthesis and capacitive property of hierarchical hollow manganese oxide nanospheres with large specific surface area. *Journal of Power Sources,* 2009. 193(2): p. 939-943.

[63] Wang, N., et al., Hydrothermal synthesis and electrochemical properties of MnO2 nanostructures. Crystal Research and Technology, 2009. 44(11): p. 1230-1234.

[64] Sui, N., et al., Large-Scale Preparation and Catalytic Properties of One-Dimensional alpha/beta-MnO2 Nanostructures. *Journal of Physical Chemistry C*, 2009. 113(20): p. 8560-8565.

[65] Yu, C., et al., A simple template-free strategy to synthesize nanoporous manganese and nickel oxides with narrow pore size distribution, and their electrochemical properties. *Advanced Functional Materials*, 2008. 18(10): p. 1544-1554.

[66] Rajeswari, J., et al., One-dimensional MoO2 nanorods for supercapacitor applications. *Electrochemistry Communications*, 2009. 11(3): p. 572-575.

[67] Donne, S.W., A.F. Hollenkamp, and B.C. Jones, Structure, morphology and electrochemical behaviour of manganese oxides prepared by controlled decomposition of permanganate. *Journal of Power Sources,* 2010. 195(1): p. 367-373.

[68] Yuan, A., et al., Textural and capacitive characteristics of MnO2 nanocrystals derived from a novel solid-reaction route. *Electrochimica Acta,* 2009. 54(3): p. 1021-1026.

[69] Wang, H.-Q., et al., Porous nano-MnO2: large scale synthesis via a facile quick-redox procedure and application in a supercapacitor. *New Journal of Chemistry,* 2011. 35(2): p. 469.

[70] Nayak, P.K. and N. Munichandraiah, Rapid sonochemical synthesis of mesoporous MnO2 for supercapacitor applications. *Materials Science and Engineering: B,* 2012. 177(11): p. 849-854.

[71] Ming, B., et al., Microwave–hydrothermal synthesis of birnessite-type MnO2 nanospheres as supercapacitor electrode materials. *Journal of Power Sources,* 2012. 198: p. 428-431.

[72] Zhang, X., et al., Rapid microwave synthesis of δ-MnO2 microspheres and their electrochemical property. *Journal of Materials Science: Materials in Electronics*, 2013. 24(7): p. 2189-2196.

[73] Zhang, X., et al., Rapid microwave-assisted hydrothermal synthesis of morphology-tuned MnO2 nanocrystals and their electrocatalytic activities for oxygen reduction. *Materials Research Bulletin,* 2013. 48(7): p. 2696-2701.

[74] Benhaddad, L., et al., Reactivity of Nanostructured MnO2 in Alkaline Medium Studied with a Microcavity Electrode: Effect of Oxidizing Agent. *Journal of Materials Science & Technology*, 2011. 27(7): p. 585-593.

[75] Kalubarme, R.S., H.S. Jadhav, and C.-J. Park, Electrochemical characteristics of two-dimensional nano-structured MnO2 for symmetric supercapacitor. *Electrochimica Acta,* 2013. 87: p. 457-465.

[76] Li, W., et al., MnO2 ultralong nanowires with better electrical conductivity and enhanced supercapacitor performances. *Journal of Materials Chemistry,* 2012. 22(30): p. 14864.

[77] Zhu, J., et al., Oxidation-etching preparation of MnO2 tubular nanostructures for high-performance supercapacitors. *ACS Appl. Mater. Interfaces*, 2012. 4(5): p. 2769-74.

[78] Yu, P., et al., Preparation and pseudo-capacitance of birnessite-type MnO2 nanostructures via microwave-assisted emulsion method. *Materials Chemistry and Physics*, 2009. 118(2-3): p. 303-307.

[79] Gong, L., X. Liu, and L. Lu, Synthesis of MnO2 nanorods from a ZnO template and their capacitive performances. *Materials Letters,* 2012. 67(1): p. 226-228.

[80] Nayak, P.K. and N. Munichandraiah, Mesoporous MnO2 synthesized by hydrothermal route for electrochemical supercapacitor studies. *Journal of Solid State Electrochemistry,* 2012. 16(8): p. 2739-2749.

[81] Xue, M., et al., Microfluidic etching for fabrication of flexible and all-solid-state micro supercapacitor based on MnO2 nanoparticles. *Nanoscale,* 2011. 3(7): p. 2703-8.

[82] Devaraj, S. and N. Munichandraiah, The effect of nonionic surfactant triton X-100 during electrochemical deposition of MnO2 on its capacitance properties. *Journal of The Electrochemical Society*, 2007. 154(10): p. A901-A909.

[83] Nagarajan, N., H. Humadi, and I. Zhitomirsky, Cathodic electrodeposition of MnOx films for electrochemical supercapacitors. *Electrochimica Acta*, 2006. 51(15): p. 3039-3045.

[84] Xue, T., et al., Electrodeposition of mesoporous manganese dioxide supercapacitor electrodes through self-assembled triblock copolymer templates. *Journal of Power Sources*, 2007. 164(2): p. 953-958.

[85] Broughton, J.N. and M.J. Brett, Variations in MnO2 electrodeposition for electrochemical capacitors. *Electrochimica Acta*, 2005. 50(24): p. 4814-4819.

[86] Prasad, K.R. and N. Miura, Potentiodynamically deposited nanostructured manganese dioxide as electrode material for electrochemical redox supercapacitors. *Journal of Power Sources*, 2004. 135(1-2): p. 354-360.

[87] Wei, J., N. Nagarajan, and I. Zhitomirsky, Manganese oxide films for electrochemical supercapacitors. *Journal of Materials Processing Technology,* 2007. 186(1-3): p. 356-361.

[88] Wu, Y.T. and C.C. Hu, Effects of electrochemical activation and multiwall carbon nanotubes on the capacitive characteristics of thick MnO2 deposits. *Journal of The Electrochemical Society*, 2004. 151(12): p. A2060-A2066.

[89] Lee, C.Y., et al., Characteristics and electrochemical performance of supercapacitors with manganese oxide-carbon nanotube nanocomposite electrodes. *Journal of The Electrochemical Society*, 2005. 152(4): p. A716-A720.

[90] Li, S., et al., Carbon spheres-assisted strategy to prepare mesoporous manganese dioxide for supercapacitor applications. *Journal of Solid State Chemistry,* 2013. 197: p. 29-37.

[91] Xiao, W., et al., Growth of single-crystal alpha-MnO2 nanotubes prepared by a hydrothermal route and their electrochemical properties. *Journal of Power Sources,* 2009. 193(2): p. 935-938.

[92] Yu, L.-L., J.-J. Zhu, and J.-T. Zhao, Three-Dimensional Network Mesoporous Nanostructured α-Manganese Dioxide with High Supercapacitive Performance: Facile, Environmental and Large-Scale Synthesis. *European Journal of Inorganic Chemistry*, 2013. 2013(21): p. 3719-3725.

[93] Zhang, X., et al., Rapid hydrothermal synthesis of hierarchical nanostructures assembled from ultrathin birnessite-type MnO2 nanosheets for supercapacitor applications. *Electrochimica Acta*, 2013. 89: p. 523-529.

[94] Cushing, B.L., V.L. Kolesnichenko, and C.J. O'Connor, Recent advances in the liquid-phase syntheses of inorganic nanoparticles. *Chemical Reviews*, 2004. 104(9): p. 3893-3946.

[95] Winsor, P.A., Binary And Multicomponent Solutions Of Amphiphilic Compounds Solubilization And Formation Structure And Theoretical Significance Of Liquid Crystalline Solutions. *Chemical Reviews*, 1968. 68(1): p. 1-&.

[96] Zhang, W., X. Qiao, and J. Chen, Synthesis of silver nanoparticles - Effects of concerned parameters in water/oil microemulsion. *Materials Science and Engineering B-Solid State Materials for Advanced Technology,* 2007. 142(1): p. 1-15.

[97] Xu, C., et al., Ultrathin amorphous manganese dioxide nanosheets synthesized with controllable width. *Chemical Communications*, 2013. 49(66): p. 7331-7333.

[98] Matei Ghimbeu, C., et al., Template-derived high surface area λ-MnO2 for supercapacitor applications. *Journal of Applied Electrochemistry,* 2013. 44(1): p. 123-132.

[99] Liu, X., et al., Synthesis of MnO2 nanorods from sawdust natural template and their electrochemical capacitive behaviors. *Materials Letters,* 2012. 79: p. 39-41.

[100] Li, X., et al., Flexible supercapacitor based on MnO2 nanoparticles via electrospinning. *Journal of Materials Chemistry A,* 2013. 1(35): p. 10103.

[101] Yuan, J., et al., Fabrication of MnO2-pillared layered manganese oxide through an exfoliation/reassembling and oxidation process. *Journal of Power Sources,* 2009. 189(2): p. 1278-1283.

[102] Omomo, Y., et al., Redoxable nanosheet crystallites of MnO2 derived via delamination of a layered manganese oxide. *Journal of the American Chemical Society*, 2003. 125(12): p. 3568-3575.

[103] Kadoma, Y., Y. Uchimoto, and M. Wakihara, Synthesis and structural study on MnO2 nanosheet material by X-ray absorption spectroscopic technique. *Journal of Physical Chemistry B*, 2006. 110(1): p. 174-177.

[104] Yan, J., et al., Preparation of exfoliated graphite containing manganese oxides with high electrochemical capacitance by microwave irradiation. *Carbon,* 2009. 47(14): p. 3371-3374.

[105] Wan, C., et al., Preparation of MnO2 nanostructures by controlled crystal growth and its pseudocapacitive properties. *Powder Technology,* 2013. 235: p. 706-711.

[106] Chu, H.-Y., et al., Preparation of MnO2/WMNT composite and MnO2/AB composite by redox deposition method and its comparative study as supercapacitive materials. *Ionics,* 2009. 16(3): p. 233-238.

[107] Zhang, X., et al., Development of redox deposition of birnessite-type MnO2 on activated carbon as high-performance electrode for hybrid supercapacitors. *Materials Chemistry and Physics*, 2012. 137(1): p. 290-296.

[108] Lei, Z., F. Shi, and L. Lu, Incorporation of MnO2-coated carbon nanotubes between graphene sheets as supercapacitor electrode. *ACS Appl. Mater. Interfaces,* 2012. 4(2): p. 1058-64.

[109] Zhang, Y., et al., MnO2@colloid carbon spheres nanocomposites with tunable interior architecture for supercapacitors. *Materials Research Bulletin*, 2014. 49: p. 448-453.

[110] Amade, R., et al., Optimization of MnO2/vertically aligned carbon nanotube composite for supercapacitor application. *Journal of Power Sources,* 2011. 196(13): p. 5779-5783.

[111] Subramanian, V., H.W. Zhu, and B.Q. Wei, Synthesis and electrochemical characterizations of amorphous manganese oxide and single walled carbon nanotube composites as supercapacitor electrode materials. *Electrochemistry Communications*, 2006. 8(5): p. 827-832.

[112] Xiao, F. and Y. Xu, Electrochemical co-deposition and characterization of MnO2/SWNT composite for supercapacitor application. *Journal of Materials Science: Materials in Electronics,* 2012. 24(6): p. 1913-1920.

[113] Tang, W., et al., A hybrid of MnO2 nanowires and MWCNTs as cathode of excellent rate capability for supercapacitors. *Journal of Power Sources,* 2012. 197: p. 330-333.

[114] Li, X. and B. Wei, Facile synthesis and super capacitive behavior of SWNT/MnO2 hybrid films. *Nano Energy,* 2012. 1(3): p. 479-487.

[115] Li, Q., et al., Structural evolution of multi-walled carbon nanotube/MnO2 composites as supercapacitor electrodes. *Electrochimica Acta,* 2012. 59: p. 548-557.

[116] Hu, L., et al., Symmetrical MnO2-Carbon Nanotube-Textile Nanostructures for Wearable Pseudocapacitors with High Mass Loading. *Acs Nano*, 2011. 5(11): p. 8904-8913.

[117] Wang, J.-G., et al., Coaxial carbon nanofibers/MnO2 nanocomposites as freestanding electrodes for high-performance electrochemical capacitors. *Electrochimica Acta*, 2011. 56(25): p. 9240-9247.

[118] Zhi, M., et al., Highly conductive electrospun carbon nanofiber/MnO2 coaxial nano-cables for high energy and power density supercapacitors. *Journal of Power Sources*, 2012. 208: p. 345-353.

[119] Dong, X.P., et al., MnO2-embedded-in-mesoporous-carbon-wall structure for use as electrochemical capacitors. *Journal of Physical Chemistry B,* 2006. 110(12): p. 6015-6019.

[120] Fischer, A.E., et al., Incorporation of homogeneous, nanoscale MnO2 within ultraporous carbon structures via self-limiting electroless deposition: Implications for electrochemical capacitors. *Nano Lett.*, 2007. 7(2): p. 281-286.

[121] Wang, J.-G., et al., Effect of temperature on the pseudo-capacitive behavior of freestanding MnO2@carbon nanofibers composites electrodes in mild electrolyte. *Journal of Power Sources*, 2013. 224: p. 86-92.

[122] Wang, J.-G., et al., A high-performance asymmetric supercapacitor based on carbon and carbon–MnO2 nanofiber electrodes. *Carbon*, 2013. 61: p. 190-199.

[123] Li, Z., et al., Flexible graphene/MnO2 composite papers for supercapacitor electrodes. *Journal of Materials Chemistry*, 2011. 21(38): p. 14706.

[124] Li, Z., et al., Synthesis of hydrothermally reduced graphene/MnO2 composites and their electrochemical properties as supercapacitors. *Journal of Power Sources,* 2011. 196(19): p. 8160-8165.

[125] Yu, G., et al., Enhancing the supercapacitor performance of graphene/MnO2 nanostructured electrodes by conductive wrapping. *Nano Lett.*, 2011. 11(10): p. 4438-42.

[126] Yu, A., A. Sy, and A. Davies, Graphene nanoplatelets supported MnO2 nanoparticles for electrochemical supercapacitor. *Synthetic Metals,* 2011. 161(17-18): p. 2049-2054.

[127] Chen, C.-Y., et al., Tightly connected MnO2–graphene with tunable energy density and power density for supercapacitor applications. *Journal of Materials Chemistry*, 2012. 22(16): p. 7697.

[128] Dong, X., et al., Synthesis of a MnO2–graphene foam hybrid with controlled MnO2 particle shape and its use as a supercapacitor electrode. *Carbon,* 2012. 50(13): p. 4865-4870.

[129] Gao, H., et al., High-performance asymmetric supercapacitor based on graphene hydrogel and nanostructured MnO2. *ACS Appl. Mater. Interfaces,* 2012. 4(5): p. 2801-10.

[130] Ge, J., et al., Facile dip coating processed graphene/MnO2 nanostructured sponges as high performance supercapacitor electrodes. *Nano Energy*, 2013. 2(4): p. 505-513.

[131] Zhao, Y.-Q., et al., MnO2/graphene/nickel foam composite as high performance supercapacitor electrode via a facile electrochemical deposition strategy. *Materials Letters*, 2012. 76: p. 127-130.

[132] Zhang, G., et al., Graphene–MnO2 nanocomposite for high-performance asymmetrical electrochemical capacitor. *Materials Research Bulletin,* 2014. 49: p. 577-583.

[133] Zhai, T., et al., 3D MnO2-graphene composites with large areal capacitance for high-performance asymmetric supercapacitors. *Nanoscale,* 2013. 5(15): p. 6790-6.

[134] Yang, W., et al., Synthesis of reduced graphene nanosheet/urchin-like manganese dioxide composite and high performance as supercapacitor electrode. *Electrochimica Acta*, 2012. 69: p. 112-119.

[135] Mao, L., et al., Nanostructured MnO2/graphene composites for supercapacitor electrodes: the effect of morphology, crystallinity and composition. *Journal of Materials Chemistry*, 2012. 22(5): p. 1845.

[136] Li, Y., et al., Improve the Supercapacity Performance of MnO2-Decorated Graphene by Controlling the Oxidization Extent of Graphene. *The Journal of Physical Chemistry C*, 2012. 116(48): p. 25226-25232.

[137] Wang, C.C., H.C. Chen, and S.Y. Lu, Manganese oxide/graphene aerogel composites as an outstanding supercapacitor electrode material. *Chemistry*, 2014. 20(2): p. 517-23.

[138] Lin, Y.-P., et al., Comparative study on nanostructured MnO2/carbon composites synthesized by spontaneous reduction for supercapacitor application. *Materials Chemistry and Physics*, 2011. 130(1-2): p. 367-372.

[139] Lei, Z., J. Zhang, and X.S. Zhao, Ultrathin MnO2 nanofibers grown on graphitic carbon spheres as high-performance asymmetric supercapacitor electrodes. *Journal of Materials Chemistry*, 2012. 22(1): p. 153.

[140] Hassan, S., et al., MnO2/carbon nanowalls composite electrode for supercapacitor application. *Journal of Power Sources*, 2014. 249: p. 21-27.

[141] Jaidev, et al., Polyaniline–MnO2 nanotube hybrid nanocomposite as supercapacitor electrode material in acidic electrolyte. *Journal of Materials Chemistry,* 2011. 21(44): p. 17601.

[142] Sathish, M., et al., MnO2 assisted oxidative polymerization of aniline on graphene sheets: Superior nanocomposite electrodes for electrochemical supercapacitors. *Journal of Materials Chemistry*, 2011. 21(40): p. 16216.

[143] Zhang, J., et al., Capacitive properties of PANI/MnO2 synthesized via simultaneous-oxidation route. *Journal of Alloys and Compounds*, 2012. 532: p. 1-9.

[144] Zang, J. and X. Li, In situ synthesis of ultrafine β-MnO2/polypyrrole nanorod composites for high-performance supercapacitors. *Journal of Materials Chemistry,* 2011. 21(29): p. 10965.

[145] Wang, Z.L., et al., Controllable template-assisted electrodeposition of single- and multi-walled nanotube arrays for electrochemical energy storage. *Sci. Rep.,* 2013. 3: p. 1204.

[146] Yoon, S.-B. and K.-B. Kim, Effect of poly(3,4-ethylenedioxythiophene) (PEDOT) on the pseudocapacitive properties of manganese oxide (MnO2) in the PEDOT/MnO2/multiwall carbon nanotube (MWNT) composite. *Electrochimica Acta*, 2013. 106: p. 135-142.

[147] Liu, R., J. Duay, and S.B. Lee, Electrochemical Formation Mechanism for the Controlled Synthesis of Heterogeneous MnO2/Poly(3,4-ethylenedioxythiophene) Nanowires. *Acs Nano,* 2011. 5(7): p. 5608-5619.

[148] Lang, X., et al., Nanoporous metal/oxide hybrid electrodes for electrochemical supercapacitors. *Nature Nanotechnology*, 2011. 6(4): p. 232-236.

[149] Si, W., et al., On chip, all solid-state and flexible micro-supercapacitors with high performance based on MnOx/Au multilayers. *Energy & Environmental Science,* 2013. 6(11): p. 3218.

[150] Tang, P.Y., et al., A metal-decorated nickel foam-inducing regulatable manganese dioxide nanosheet array architecture for high-performance supercapacitor applications. *Nanoscale,* 2013. 5(17): p. 8156-63.

[151] Li, Q., et al., Design and synthesis of MnO(2)/Mn/MnO(2) sandwich-structured nanotube arrays with high supercapacitive performance for electrochemical energy storage. Nano Lett, 2012. 12(7): p. 3803-7.

[152] Cao, J., et al., High-performance flexible supercapacitor electrodes based on Te nanowire arrays. *Journal of Materials Chemistry A,* 2013. 1(34): p. 10024.

[153] Sherrill, S.A., et al., MnO2/TiN heterogeneous nanostructure design for electrochemical energy storage. *Phys. Chem. Chem. Phys.,* 2011. 13(33): p. 15221-6.

[154] Hwang, S.-G., et al., Behavior of NiO–MnO2/MWCNT composites for use in a supercapacitor. *Materials Chemistry and Physics*, 2011. 130(1-2): p. 507-512.

[155] Li, Q., et al., Synthesis and electrochemical performance of multi-walled carbon nanotube/polyaniline/MnO2 ternary coaxial nanostructures for supercapacitors. *Journal of Power Sources*, 2011. 196(1): p. 565-572.

[156] Yang, H., et al., Influences of graphene oxide support on the electrochemical performances of graphene oxide-MnO2 nanocomposites. *Nanoscale Res. Lett.,* 2011. 6: p. 531.

[157] Cheng, Y., et al., Synergistic effects from graphene and carbon nanotubes enable flexible and robust electrodes for high-performance supercapacitors. *Nano Lett.,* 2012. 12(8): p. 4206-11.

[158] Kim, K.-S. and S.-J. Park, Synthesis and high electrochemical performance of polyaniline/MnO2-coated multi-walled carbon nanotube-based hybrid electrodes. Journal of Solid State *Electrochemistry*, 2012. 16(8): p. 2751-2758.

[159] Zhao, H., et al., The capacitive properties of amorphous manganese dioxide electrodeposited on different thermally-treated carbon papers. *Electrochimica Acta*, 2013. 91: p. 50-57.

[160] Xiong, G., et al., MnO2-coated graphitic petals for supercapacitor electrodes. *Journal of Power Sources*, 2013. 227: p. 254-259.

[161] Wang, T., et al., MnO nanoparticle@mesoporous carbon composites grown on conducting substrates featuring high-performance lithium-ion battery, supercapacitor and sensor. *Sci. Rep.,* 2013. 3: p. 2693.

[162] Zhao, J., et al., Flexible hierarchical nanocomposites based on MnO2 nanowires/CoAl hydrotalcite/carbon fibers for high-performance supercapacitors. *RSC Advances*, 2013. 3(4): p. 1045.

[163] Xiao, X.-Z. and Q.-F. Yi, Synthesis and Electrochemical Capacity of MnO2/SMWCNT/PANI Ternary Composites. *Journal of Inorganic Materials,* 2013. 28(8): p. 825-830.

[164] Wang, H., et al., Design, synthesis and the electrochemical performance of MnO2/C@CNT as supercapacitor material. *Materials Research Bulletin,* 2013. 48(9): p. 3389-3393.

[165] Tao, J., et al., Solid-state high performance flexible supercapacitors based on polypyrrole-MnO2-carbon fiber hybrid structure. *Sci. Rep.,* 2013. 3: p. 2286.

[166] Li, J., T. Que, and J. Huang, Synthesis and characterization of a novel tube-in-tube nanostructured PPy/MnO2/CNTs composite for supercapacitor. *Materials Research Bulletin,* 2013. 48(2): p. 747-751.

[167] Reddy, A.L.M., et al., Multisegmented Au-MnO2/Carbon Nanotube Hybrid Coaxial Arrays for High-Power Supercapacitor Applications. *Journal of Physical Chemistry C,* 2010. 114(1): p. 658-663.

[168] Yu, L., et al., Hierarchical NiCo2O4@MnO2 core-shell heterostructured nanowire arrays on Ni foam as high-performance supercapacitor electrodes. *Chem. Commun.* (Camb), 2013. 49(2): p. 137-9.

[169] Xin Zhang, Y., F. Li, and M. Huang, One-step hydrothermal synthesis of hierarchical MnO2-coated CuO flower-like nanostructures with enhanced electrochemical properties for supercapacitor. *Materials Letters,* 2013. 112: p. 203-206.

[170] Kang, J., et al., Enhanced supercapacitor performance of MnO2 by atomic doping. *Angew. Chem. Int. Ed. Engl.,* 2013. 52(6): p. 1664-7.

[171] Su, D.S. and R. Schloegl, Nanostructured Carbon and Carbon Nanocomposites for Electrochemical Energy Storage Applications. *Chemsuschem.*, 2010. 3(2): p. 136-168.

[172] Dubal, D.P., W.B. Kim, and C.D. Lokhande, Galvanostatically deposited Fe: MnO2 electrodes for supercapacitor application. *Journal of Physics and Chemistry of Solids,* 2012. 73(1): p. 18-24.

[173] Dubal, D.P. and C.D. Lokhande, Significant improvement in the electrochemical performances of nano-nest like amorphous MnO2 electrodes due to Fe doping. *Ceramics International*, 2013. 39(1): p. 415-423.

[174] Kim, H. and B.N. Popov, Synthesis and characterization of MnO2-based mixed oxides as supercapacitors. *Journal of The Electrochemical Society,* 2003. 150(3): p. D56-D62.

[175] Chen, Y.S. and C.C. Hu, Capacitive characteristics of binary manganese-nickel oxides prepared by anodic deposition. *Electrochemical and Solid State Letters*, 2003. 6(10): p. A210-A213.

[176] Prasad, K.R. and N. Miura, Electrochemically synthesized MnO2-based mixed oxides for high performance redox supercapacitors. *Electrochemistry Communications*, 2004. 6(10): p. 1004-1008.

[177] Simon, P. and Y. Gogotsi, Materials for electrochemical capacitors. *Nature Materials*, 2008. 7(11): p. 845-854.

[178] Nam, K.-W., M.G. Kim, and K.-B. Kim, In situ MnK-edge X-ray absorption spectroscopy studies of electrodeposited manganese oxide films for electrochemical capacitors. *Journal of Physical Chemistry C,* 2007. 111(2): p. 749-758.

[179] Ataherian, F. and N.-L. Wu, Long-Term Charge/Discharge Cycling Stability of MnO2 Aqueous Supercapacitor under Positive Polarization. *Journal of The Electrochemical Society*, 2011. 158(4): p. A422.

[180] Beguin, F., V. Khomenko, and E. Raymundo-Pinero, Optimisation of an asymmetric manganese oxide/activated carbon capacitor working at 2V in aqueous medium. *Journal of Power Sources*, 2006. 153(1): p. 183-90.

[181] Wang, C.-H., H.-C. Hsu, and J.-H. Hu, High-energy asymmetric supercapacitor based on petal-shaped MnO2 nanosheet and carbon nanotube-embedded polyacrylonitrile-based carbon nanofiber working at 2 V in aqueous neutral electrolyte. *Journal of Power Sources*, 2014. 249: p. 1-8.

[182] Brousse, T. and D. Belanger, A hybrid Fe3O4-MnO2 capacitor in mild aqueous electrolyte. *Electrochemical and Solid State Letters*, 2003. 6(11): p. A244-A248.

[183] Luo, J.-Y., et al., A novel LiTi2(PO4)(3)/MnO2 hybrid supercapacitor in lithium sulfate aqueous electrolyte. *Electrochimica Acta,* 2008. 53(28): p. 8128-8133.

[184] Khomenko, V., et al., High-voltage asymmetric supercapacitors operating in aqueous electrolyte. Applied *Physics a-Materials Science & Processing,* 2006. 82(4): p. 567-573.

[185] Qu, Q.T., et al., A new cheap asymmetric aqueous supercapacitor: Activated carbon//NaMnO2. *Journal of Power Sources*, 2009. 194(2): p. 1222-1225.

[186] Qu, Q., et al., A cheap asymmetric supercapacitor with high energy at high power: Activated carbon//K0.27MnO2·0.6H(2)O. *Journal of Power Sources,* 2010. 195(9): p. 2789-2794.

[187] Yeager, M., et al., Highly Efficient K0.15MnO2Birnessite Nanosheets for Stable Pseudocapacitive Cathodes. *The Journal of Physical Chemistry C,* 2012. 116(38): p. 20173-20181.

[188] Lin, Y.-P. and N.-L. Wu, Characterization of MnFe2O4/LiMn2O4 aqueous asymmetric supercapacitor. *Journal of Power Sources*, 2011. 196(2): p. 851-854.

[189] Wang, Y.G. and Y.Y. Xia, A new concept hybrid electrochemical surpercapacitor: Carbon/LiMn2O4 aqueous system. *Electrochemistry Communications,* 2005. 7(11): p. 1138-1142.

[190] Yu, H., et al., Application of a novel redox-active electrolyte in MnO2-based supercapacitors. *Science China Chemistry,* 2012. 55(7): p. 1319-1324.

[191] Shi, S., et al., Flexible supercapacitors. *Particuology,* 2013. 11(4): p. 371-377.

[192] Hu, L. and Y. Cui, Energy and environmental nanotechnology in conductive paper and textiles. *Energy & Environmental Science*, 2012. 5(4): p. 6423-6435.

[193] Hu, L., H. Wu, and Y. Cui, Printed energy storage devices by integration of electrodes and separators into single sheets of paper. *Applied Physics Letters,* 2010. 96(18).

[194] Hu, L., et al., Thin, Flexible Secondary Li-Ion Paper Batteries. *Acs Nano,* 2010. 4(10): p. 5843-5848.

[195] Nyholm, L., et al., Toward Flexible Polymer and Paper-Based Energy Storage Devices. *Advanced Materials*, 2011. 23(33): p. 3751-3769.

[196] Bao, L., J. Zang, and X. Li, Flexible Zn2SnO4/MnO2 Core/Shell Nanocable-Carbon Microfiber Hybrid Composites for High-Performance Supercapacitor Electrodes. *Nano Lett.,* 2011. 11(3): p. 1215-1220.

[197] Chen, Y.-C., et al., Highly flexible supercapacitors with manganese oxide nanosheet/carbon cloth electrode. *Electrochimica Acta*, 2011. 56(20): p. 7124-7130.

[198] Kang, Y.J., et al., Fabrication and characterization of flexible and high capacitance supercapacitors based on MnO2/CNT/papers. *Synthetic Metals,* 2010. 160(23-24): p. 2510-2514.

[199] Kim, J.-H., et al., Synthesis and Electrochemical Properties of Spin-Capable Carbon Nanotube Sheet/MnOx Composites for High-Performance Energy Storage Devices. *Nano Lett.,* 2011. 11(7): p. 2611-2617.

[200] Lei, Z., F. Shi, and L. Lu, Incorporation of MnO2-Coated Carbon Nanotubes between Graphene Sheets as Supercapacitor Electrode. ACS *Appl. Mater. Interfaces,* 2012. 4(2): p. 1058-1064.

[201] Lu, X., et al., WO3-x@Au@MnO2 Core-Shell Nanowires on Carbon Fabric for High-Performance Flexible Supercapacitors. *Advanced Materials,* 2012. 24(7): p. 938-+.

[202] Yu, G., et al., Solution-Processed Graphene/MnO2 Nanostructured Textiles for High-Performance Electrochemical Capacitors. *Nano Lett.,* 2011. 11(7): p. 2905-2911.

[203] Yuan, L., et al., Flexible Solid-State Supercapacitors Based on Carbon Nanoparticles/MnO2 Nanorods Hybrid Structure. *Acs Nano*, 2012. 6(1): p. 656-661.

[204] Shi, S., et al., Flexible asymmetric supercapacitors based on ultrathin twodimensional nanosheets with outstanding electrochemical performance and aesthetic property (vol 3, 2598, 2013). *Sci. Rep.,* 2014. 4.

[205] Su, Z., et al., Co-electro-deposition of the MnO2–PEDOT:PSS nanostructured composite for high areal mass, flexible asymmetric supercapacitor devices. *Journal of Materials Chemistry A,* 2013. 1(40): p. 12432.

[206] Sen, P., et al., Conducting polymer based manganese dioxide nanocomposite as supercapacitor. *Electrochimica Acta,* 2013. 108: p. 265-273.

[207] Brousse, T., M. Toupin, and D. Belanger, A hybrid activated carbon-manganese dioxide capacitor using a mild aqueous electrolyte. *Journal of The Electrochemical Society,* 2004. 151(4): p. A614-A622.

[208] Brousse, T., et al., Long-term cycling behavior of asymmetric activated carbon/MnO2 aqueous electrochemical supercapacitor. *Journal of Power Sources,* 2007. 173(1): p. 633-641.

[209] Qu, Q., et al., Electrochemical Performance of MnO2 Nanorods in Neutral Aqueous Electrolytes as a Cathode for Asymmetric Supercapacitors. *Journal of Physical Chemistry C*, 2009. 113(31): p. 14020-14027.

[210] Shen, C., et al., A high-energy-density micro supercapacitor of asymmetric MnO2–carbon configuration by using micro-fabrication technologies. *Journal of Power Sources*, 2013. 234: p. 302-309.

[211] Khomenko, V., E. Raymundo-Pinero, and F. Beguin, Optimisation of an asymmetric manganese oxide/activated carbon capacitor working at 2 V in aqueous medium. *Journal of Power Sources,* 2006. 153(1): p. 183-190.

[212] Chen, L., et al., Facile fabrication of mesoporous manganese oxides as advanced electrode materials for supercapacitors. *Journal of Solid State Electrochemistry*, 2013. 17(10): p. 2579-2588.

[213] Zhang, X., et al., High performance asymmetric supercapacitor based on MnO2 electrode in ionic liquid electrolyte. *Journal of Materials Chemistry A*, 2013. 1(11): p. 3706.

[214] Chen, H., et al., One-Step Fabrication of Ultrathin Porous Nickel Hydroxide-Manganese Dioxide Hybrid Nanosheets for Supercapacitor Electrodes with Excellent Capacitive Performance. *Advanced Energy Materials,* 2013. 3(12): p. 1636-1646.

[215] Chang, J., et al., Asymmetric Supercapacitors Based on Graphene/MnO2Nanospheres and Graphene/MoO3Nanosheets with High Energy Density. *Advanced Functional Materials*, 2013. 23(40): p. 5074-5083.

[216] Chen, L.F., et al., Bacterial-cellulose-derived carbon nanofiber@MnO(2) and nitrogen-doped carbon nanofiber electrode materials: an asymmetric supercapacitor with high energy and power density. *Adv. Mater.,* 2013. 25(34): p. 4746-52.

[217] Sawangphruk, M., et al., High-performance supercapacitor of manganese oxide/reduced graphene oxide nanocomposite coated on flexible carbon fiber paper. *Carbon*, 2013. 60: p. 109-116.

[218] Chen, P.-C., et al., Preparation and Characterization of Flexible Asymmetric Supercapacitors Based on Transition-Metal-Oxide Nanowire/Single-Walled Carbon Nanotube Hybrid Thin-Film Electrodes. *Acs Nano*, 2010. 4(8): p. 4403-4411.

[219] Shao, Y., et al., High-performance flexible asymmetric supercapacitors based on 3D porous graphene/MnO2 nanorod and graphene/Ag hybrid

thin-film electrodes. *Journal of Materials Chemistry C*, 2013. 1(6): p. 1245.

[220] Jin, Y., et al., Graphene-patched CNT/MnO2 nanocomposite papers for the electrode of high-performance flexible asymmetric supercapacitors. *ACS Appl. Mater. Interfaces*, 2013. 5(8): p. 3408-16.

[221] Moser, F., et al., Transparent electrochemical capacitor based on electrodeposited MnO2 thin film electrodes and gel-type electrolyte. *Electrochemistry Communications,* 2009. 11(6): p. 1259-1261.